Journal of
Materials Chemistry C

Accepted Manuscript

Development of n-Type Organic Semiconductors for Thin Film Transistors: A Viewpoint of Molecular Design

Xike Gao*, and Yunbin Hu

Laboratory of Materials Science, Shanghai Institute of Organic Chemistry, Chinese Academy of Sciences, 345 Lingling Road, Shanghai 200032, China

*Corresponding author. E-mail: gaoxk@mail.sioc.ac.cn

Abstract

The past ten years have witnessed great progress of n-type organic semiconductors (OSCs) for organic thin film transistors (OTFTs), while the device performance and ambient stability of n-type OSCs are still outmatched by their p-type counterparts. The pursuit of high-performance ambient-stable n-type OSCs for OTFTs is highly desirable for realizing robust, large-area and low-cost organic integrate circuits. In this feature article, we'll review the development of n-type OSCs for OTFTs from a viewpoint of molecular design, where more than nine molecular design strategies with > 120 representative n-type OSCs were summarized and analyzed to give some valuable insights for this significant but challenging field.

1. Introduction

As an important branch of organic electronics, organic thin film transistors (OTFTs) have attracted more and more attention for their applications in low-cost, large-area and flexible electronic products, such as flexible active-matrix displays, organic tags/memories, and chemical/biological sensors.[1,2] Organic semiconductors (OSCs) are the active components of OTFTs and can be divided into p-type (hole-transporting) and n-type (electron-transporting) ones. Now, the performance of n-type OSCs is outmatched by that of the burgeoning p-type counterparts.[3,4] For example, some solution-processed p-type small molecular and polymeric semiconductors have shown hole mobilities larger than 30 and 10 $cm^2 V^{-1} s^{-1}$, respectively.[5–7] However, there are still few n-type OSCs that could be compared with the performance of amorphous silicon TFTs (mobility: ~1.0 $cm^2 V^{-1} s^{-1}$), with unsatisfied device air stability.[3,4] Since both p- and n-type OSCs with comparable performance are required for ambipolar transistors, p-n junctions and organic complementary circuits,[2,8] the development of high-performance ambient-stable n-type OSCs for OTFTs are highly desirable.

There is no clear boundary between p- and n-type OSCs, since field-effect (FET) electron mobilities have been generally observed in a number of common p-type polymers, such as poly(3-hexylthiophene) (P3HT) and poly(*p*-phenylenevinylene) (PPV), by using an appropriate hydroxyl-free gate dielectric and low-work-function electrodes.[9] To decrease the trapping of electrons at the semiconductor–dielectric interface induced by hydroxyl groups and guarantee suitable molecular packing for charge carrier transport, the self-assembling monolayers (SAMs) of

octadecyltrichlorosilane (OTS-18), hexamethyldisilazane (HMDS), octadecyltrimethoxysilane (OTMS) or other modifying reagents on substrates are widely used for fabricating OTFTs.[10] n-type OSCs are commonly electron-deficient small molecular and polymeric π-conjugated systems with the lowest unoccupied molecular orbital (LUMO) levels below –3.0 eV.[11] Although the LUMO energy levels of most n-type OSCs are higher than –4.0 eV, the high work-function electrodes such as Au (5.1 eV) are still commonly used due to their much better environmental stability compared with the low work-function electrodes (Ca, Mg, Al etc). This high injection barrier could be solved by the electrode modifications and the electrode–semiconductor interface engineering.[12] Since the first observation of n-channel OTFTs by using lutetium and thulium bisphthalocyanines as semiconductors in 1990,[13] significant progresses in the field of n-type OSCs and n-channel OTFTs have been made and the results could be obtained from the recent reviews.[3,4,11,14–20] In 2004, Newman and co-workers[11] wrote an impressive review on OTFTs and n-type OSCs, and especially highlighted the molecular design for n-type OSCs. Over the past decade, hundreds of n-type OSCs for OTFTs have been synthesized with many efficient molecular design strategies. In this feature article, we'll discuss the progress in recent ten years on n-type OSCs for OTFTs from a viewpoint of molecular design.

2. Basic overview for designing n-type OSCs for OTFTs

Compounds **1**–**6** (Scheme 1) are the representative n-type OSCs early developed for OTFTs and could illustrate the basic molecular design strategy. High electron

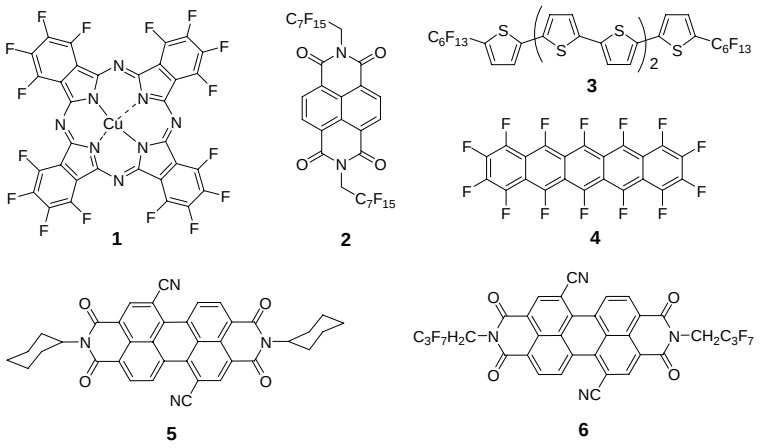

Scheme 1. Representative early stage n-type OSCs for transistors

mobility, good processability, and excellent ambient/operating device stability are the key targets for the molecular design of n-type OSCs, of which the ambient/operating device stability is the most challenging topic for n-type OSCs used in OTFTs due to the vulnerable electron charge carriers that are easily trapped by ambient species, such as O_2 and H_2O.[21] For example, vacuum-deposited bottom-gate top-contact (BGTC) OTFTs based on a naphthalene diimide (NDI) derivative bearing *N*-cyclohexyl groups exhibited an electron mobility (μ_e) of up to 6.2 $cm^2\,V^{-1}\,s^{-1}$ under a positive argon atmosphere, however, when tested in air the μ_e value was degraded to 0.41 $cm^2\,V^{-1}\,s^{-1}$ with a three-order lower current on/off ratios ($I_{on/off}$).[22] What factors affect the ambient/operating device stability of n-type OSCs for OTFTs? Generally, both the energetic (thermodynamic) factors and the kinetic elements influence the stability of n-type OSCs in OTFTs. For the energetic factors, the LUMO energy levels of n-type OSCs should be less than or equal to –4.0 eV (a value between –4.3 and –4.4 will be better) for ambient stable electron injection and transport in OTFTs.[23–26] For example, solution-processed BGTC OTFTs based on a fullerene derivative [84]PCBM showed an electron mobility (μ_e) of 0.5×10^{-3} $cm^2\,V^{-1}\,s^{-1}$ under ambient light in air and could

continue to operate even after exposure to air for several months without any noticeable degradation.[27] The low-lying LUMO energy level of [84]PCBM (about −4.0 eV) should be the key energetic factor for the device air stability,[27] since most fullerene derivatives have the higher LUMO energies (such as [60]PCBM, about −3.7 eV) and could only perform as n-channel transistors in vacuum or in inert atmosphere.[27] Copper hexadecafluorophthalocyanine (F_{16}CuPc, **1**) reported by Bao *et al* in 1998 is the early ambient stable n-type OSC, its BGTC OTFTs showed an electron mobility of 0.03 $cm^2 V^{-1} s^{-1}$ with long-term device stability in air.[28] The deep LUMO energy level (about −4.3 eV estimated from the Cyclic Voltammetry results)[24] and the fluorine atoms that could block moisture from penetrating through the films are respectively the energetic and kinetic factors for device stability.[28] The kinetic factors that influence the n-channel OTFT stability were systematically studied by Katz *et al* in 2000,[29,30] where OTFTs based on a NDI derivative that bears two fluorinated chains (**2**) showed electron mobility of up to 0.1 $cm^2 V^{-1} s^{-1}$ with good air stability, while those with alkyl chains showed no FET activity in air.[29,30] Since the *N*-fluororalkyl groups only slightly depress the LUMO energy level of **2** ($\Delta E \leq 0.15$ eV) relative to the alkyl chain functionalized NDIs, with the help of single crystal analysis, Katz *et al.* proposed that a kinetic barrier formed by the densely packed R^F groups could hinder the ambient species (O_2, H_2O) penetration and contribute to the electron-transport air stability.[29] Besides the microstructure of thin films, the thin film morphology (crystallinity, grain size, and grain boundaries) and active layer thickness are all kinetic factors that influence the n-channel OTFT stability.[31–33] Thin films with

high crystallinity, large grain size, and low density of grain boundaries favor the device air stability.

There is interplay between the energetic and kinetic factors on ambient stability of n-channel OTFTs,[33] they oppose each other also complement each other. α,ω-Diperfluorohexylsexithiophene **3**[34] and perfluoropentacene **4**[35] both have fluorinated groups that might be served as the kinetic factors for device stability. However, BGTC OTFTs based on **3** and **4** only showed n-channel behaviors in N_2 atmosphere or in vacuum with the electron mobility of up to 0.02 and 0.11 $cm^2 V^{-1} s^{-1}$, respectively.[34,35] The device air instability might be explained by the high LUMO energy levels of **3** and **4** (–2.9 and –3.65 eV, respectively),[34,35] and the energetic factors rather than the kinetic elements dominate the n-channel device stability of **3** and **4**. Core-cyanated perylene diimides (PDI) derivative **5**[36] is the early example designed in viewpoint of energetic factors, the deep LUMO energy of –4.33 eV realized by the introduction of two electron-withdrawing cyano groups on the PDI core is responsible for the ambient stability of n-channel OTFTs of **5** (μ_e: ~0.1 $cm^2 V^{-1} s^{-1}$ in air for BGTC device).[36] Both the energetic and kinetic factors play an important role in improving the electron mobility and device stability of OTFTs based on a *N*-fluoroalkyl functionalized dicyano-PDI derivative (**6**).[36] Vacuum-deposited BGTC OTFTs based on **6** exhibited electron mobility as high as 0.64 $cm^2 V^{-1} s^{-1}$ with current on/off ratio ($I_{on/off}$) of 10^4, and the devices showed excellent ambient stability with negligible degradation in mobility, threshold voltage (V_T), and $I_{on/off}$ over six months.[36] The device ambient stability of **6** is owing to its low-lying LUMO energy

level (–4.44 eV) and a kinetic barrier formed by the short π–π interactions and the densely packed fluorinated *N*-groups.[36] The spin-coated bottom-gate bottom-contact (BGBC) OTFTs based on **6** exhibited electron mobilities of up to 0.15 $cm^2 V^{-1} s^{-1}$ in vacuum and 0.14 $cm^2 V^{-1} s^{-1}$ in air with $I_{on/off} > 10^3$, and mobilities of ~0.08 $cm^2 V^{-1} s^{-1}$ were still measured after 20 days of continuous exposure to air.[37] By using an improved solution processing technique and triethoxy-*1H,1H,2H,2H*-tridecafluoro-n-octylsilane SAMs for substrate treatments, highly crystallized thin films of **6** were achieved, and BGTC OTFTs based on these crystalline films showed electron mobility of up to 1.3 $cm^2 V^{-1} s^{-1}$ and $I_{on/off}$ of 10^5, with excellent device air stability.[38] In addition, single-crystal field-effect transistors (SCFETs) of **6** were also studied with electron mobilities of up to 6 $cm^2 V^{-1} s^{-1}$ in vacuum and 3 $cm^2 V^{-1} s^{-1}$ in air.[39] Band-like electron transport in vacuum-gap SCFETs of **6** was observed recently with electron mobility of up to 10.8 $cm^2 V^{-1} s^{-1}$ when measured at low temperature (230 K) in vacuum.[40] The mobility deviations from the values measured in vacuum to those tested in air demonstrate some air sensibility of **6**-based SCFETs,[39] similar phenomena were also observed for vacuum-deposited BGTC OTFTs based on **6** and other *N*-fluoroalkyl functionalized dicyano-PDI derivatives.[41] The results demonstrate that the energetic and kinetic factors could not fully explain the ambient stability of n-channel OTFTs, and further efforts are required for clarifying the mechanism of electron-transport stability.

3. The strategies for designing n-type OSCs for OTFTs

By summarizing recent ten years' references on n-type OSCs for OTFTs, we present

here more than nine molecular-design strategies toward high-performance ambient-stable n-channel OTFTs. In each section, the n-type OSCs with electron mobility larger than 0.5 $cm^2 V^{-1} s^{-1}$ for vacuum-deposited OTFTs and $\mu_e > 0.1$ $cm^2 V^{-1} s^{-1}$ for solution-processed n-type OSCs are highlighted (see Table 1 for details), as well as the very stable OSCs for n-channel OTFTs. The HOMO/LUMO energy levels' control of n-type OSCs is another emphasis in the following sections.

Table 1. Device performance of the representative n-type OSCs for OTFTs with molecular orbital energy values [a]

	HOMO/LUMO energy (eV)	Optimized μ_e ($cm^2V^{-1}s^{-1}$) ()[b]	$I_{on/off}$	V_T (V)	Device structure	Ref.
6	–6.8/–4.5	0.64 (v-d, air) 1.3 (s-d, air) 6 (s-c, vacuum) 3 (s-c, air)	10^4 10^5 10^3–10^4		BGTC (Au) BGBC (Au)	36 38 39
7	–6.71/–3.71	0.7 (v-d, air)	10^5–10^6	3–13	BGTC (Au)	44
8		0.57 (v-d, air)	10^7	13–48	BGTC (Au)	45
12	/–3.85	1.44 (v-d, N_2) 1.24 (v-d, air)	10^6	39–47 47–57	BGTC (Au)	49
13	/–3.79	0.62 (v-d, N_2) 0.37 (v-d, air)	10^6–10^7	21–29 28–39	BGTC (Au)	49
24[c]	–6.13/–3.90	1.0 (s-d, N_2) 0.51 (s-d, air)	10^4–10^5 10^3–10^4	4 –15	BGTC (Au)	61
25	–5.88/–4.04	0.16 (s-d, air)	10^6	23	TGBC (Au)	62
27	/–4.23	0.91 (v-d, N_2) 0.82 (v-d, air)	10^7–10^8	28	BGTC (Au)	63
33	/–3.88	0.66 (v-d, N_2) 0.61 (v-d, air)	10^6	9–15 11–29	BGTC (Au)	49 69
34	/–3.94	0.85 (v-d, N_2) 0.51 (v-d, air)	10^7	8–14 17–41	BGTC (Au)	49
38	–6.92/–4.01	0.86 (v-d, N_2) 0.91 (v-d, air) 0.95 (s-d, air) 8.6 (s-c, air)	10^5–10^6 10^5 10^7	20±1 25±2 6±4 9	BGTC (Au)	71 72 73
39	–6.92/–4.01	1.26 (v-d, N_2) 1.43 (v-d, air)	10^7	15±2 23±2	BGTC (Au)	71
45	–6.1/–3.9	0.15 (s-d, N_2)	10^6	8	BGTC (Au)	78

47	–5.36/–3.91	0.85 (s-d, air)	10^6–10^7	5–10	TGBC (Au)	80
48	–5.4/–4.0	0.2 (s-d, air) 0.5 (s-d, air)	10^3 10^5		BGTC (Au) TGBC (Au)	81
53[c]	–5.62/–3.90 –5.42/–4.0	1.57 (s-d, air) 1.8 (s-d, N_2)	10^4 10^6	 13	TGBC (Au) TGBC (Cs_2CO_3/Au)	86 87
54[c]	–5.90/–3.90	0.24 (s-d, N_2)	10^6	12	BGTC (Au)	89
55	–5.45/–3.80	0.30 (s-d, N_2)	10^5–10^6		BGTC (Ag)	90
56[c]	–5.38/–3.66	3.0 (s-d, N_2)			TGBC (Au)	91
57[c]	–5.65/–4.18	2.36 (s-d, N_2)			BGTC (Au)	92
58	–5.84/–4.32	0.16 (s-d, air)	10^8	5	BGTC (Au)	25
61	–5.4/–3.7	1.5 (s-d, N_2)		13	TGBC (Au)	95
62	–5.9/–3.8	0.14 (s-d, N_2)		12	TGBC (Au)	95
63	–5.7/–3.8	0.21 (s-d, N_2)		9	TGBC (Au)	95
64	/–3.8	0.17 (s-d, N_2)	10^4	2	TGBC (Au)	96
65	–6.4/–4.3	0.51 (s-d, air) 0.55 (s-d, air) 0.65 (s-d, air) 0.30 (s-d, air)	10^6–10^7 10^6 10^8 10^8	2–9 9 –2 4	BGTC (Ag) BGTC (Au) BGBC (Au) TGBC (Au)	97 102
66	–6.45/–4.36	0.18 (s-d, air) 0.34 (s-d, air) 0.11 (s-d, air)	10^7 10^7 10^6	6 0 9	BGTC (Au) BGBC (Au) TGBC (Au)	102
67	–6.46/–4.38	2.62 (s-d, air) 3.50 (s-d, air) 1.21 (s-d, air)	10^7 10^8 10^9	5 0 5	BGTC (Au) BGBC (Au) TGBC (Au)	102
68	–6.44/–4.36	0.25 (s-d, air) 0.25 (s-d, air) 0.0009 (s-d, air)	10^7 10^7 10^4	5 3 8	BGTC (Au) BGBC (Au) TGBC (Au)	102
69	–6.43/–4.32	0.70 (s-d, air)	10^7	7	BGTC (Au)	99
76	–6.53/–4.43	0.14 (s-d, air)	10^3	10	BGTC (Au)	100
78	/–4.2	0.16 (s-d, air)	10^3		BGTC (Au)	117
81	–6.1/–4.3	0.90 (s-d, air)	10^5		BGTC (Au)	120
82	–5.61/–4.31	0.22 (s-d, air)	10^4–10^5	3–13	BGTC (Au)	121
83	–6.24/–4.51	0.55 (v-d, air)	10^6	10	BGTC (Au)	122
84	–6.23/–4.51	0.35 (s-d, air)	10^5–10^6	–1	BGTC (Au)	122
85	–5.7/–4.2	0.5 (s-d, air)	10^3	10	TGBC (Au)	123
86	–6.0/–4.2	0.10 (linear, s-d, air) 0.03 (s-d, air)	 10^5		BGBC (Au)	124
94	–5.3/–3.7	0.12 (s-d, N_2)	10^5–10^6	21	BGTC (Au)	133
100	–6.6/–3.8	0.34 (s-d, N_2)	10^4	8	TGBC (Au)	134
102	–6.28/–3.47	0.19 (s-d, vacuum)	10^5	76	TGBC (Au)	136
104	–6.12/–4.10	1.1 (s-d, air) 0.1 (s-d, air)			TGBC (Au) BGTC (Au)	137

106	–6.98/–4.14	0.55 (s-c, N_2)	10^5	45	BGTC (Au)	139
107	–6.04/–4.22	4.65 (s-c, air) 0.11 (s-d, air)			BGTC (Ag) BGTC (Au)	140 141
108	–6.14/–4.30	0.70 (s-d, air)	10^7	21	BGTC (Au)	141
109	–6.16/–4.26	0.25 (s-d, air)	10^7		BGTC (Au)	142
110	–6.08/–4.40	0.18 (s-d, air)	10^5	0.95	BGTC (Au)	143
118	–5.75/–4.01	3.3 (v-d, vacuum) 0.5 (v-d, air) 2.5 (s-d, vacuum)	10^5 10^5		BGTC (Au)	154 155
119	–6.45/–3.79	3.39 (s-c, air)	10^4		TGTC (graphite)	156

[a] v-d: vacuum deposition, v-d: solution deposition, s-c: single crystal, BGTC: bottom-gate top-contact, BGBC: bottom-gate bottom-contact, TGBC: top-gate bottom-contact, TGTC: top-gate top-contact. [b] The device depositing and testing conditions. [c] Ambipolar transporting features were observed.

3.1 The functionalization of electron-deficient π-conjugated systems by using fluorine or fluorocarbon-based functional groups, a kinetic mechanism

Compounds **7**–**19** are shown in Scheme 2 to illustrate molecular design strategy in this section. 1,4,5,8-Naphthalene diimides (NDIs)[42] are a class of electron-deficient π-functional molecules with low-lying HOMO/LUMO levels (–7.0/–3.4 eV for a model NDI molecule with *N*-methyl groups estimated by DFT calculations).[43] As mentioned in section 2, Katz et al.[29] reported ambient-stable n-channel OTFTs based on a fluorocarbon-functionalized NDI derivative **2** with μ_e of up to 0. 1 $cm^2 V^{-1} s^{-1}$. Since the fluorocarbon-based *N*-groups depress the LUMO energy level of **2** slightly ($\Delta E \leq 0.15$ eV), a kinetic barrier formed by the densely packed fluoroalkyl chains was proposed and it could hinder the ambient species (O_2, H_2O) penetration and contribute to the electron-transport air stability.[29] Later on, a series of *N*-fluorocarbon (R^F)-functionalized NDI derivatives **7**–**10** were designed and synthesized for

ambient-stable n-channel OTFTs.[44–47] A *N*,*N*′-bis(3-(perfluoroctyl)propyl)-NDI derivative **7** was reported by Katz and coworkers,[44] **7**-based BGTC OTFTs showed μ_e approaching 0.7 $cm^2 V^{-1} s^{-1}$ in air ($I_{on/off}$: 10^5–10^6 and V_T: 3–13 V),[44] which is much better in performance than **2**-based devices.[29] In addition, the electrical stability against gate bias stress of **7**-based devices is comparable to that of a-Si TFTs.[44] The results demonstrate that *N*-$(CH_2)_3C_8F_{17}$ group is more powerful than *N*-$CH_2C_7F_{15}$ substituent for achieving high-performance NDI-based n-type OSCs. NDI derivatives bearing perfluoroalkyl benzyl *N*-groups were readily synthesized from commercially available starting materials, of which compound **8** presented μ_e values of up to 0.57 $cm^2 V^{-1} s^{-1}$ in air for its BGTC OTFTs with the $I_{on/off}$ as high as 10^8.[45] Low-temperature-deposited, transparent, and ambient-operable n-channel OTFTs were demonstrated by Katz *et al.* by using fluorinated phenylethylated NDI derivatives as active layers.[46] The devices based on **9** showed μ_e values of 0.1–0.31 $cm^2 V^{-1} s^{-1}$ in air with the depositing substrate temperature ≤ 80 °C, and the optimized mobility for a flexible and transparent transistor of **9** was 0.23 $cm^2 V^{-1} s^{-1}$ with low hysteresis.[46] BGTC OTFTs based on a 3,5-bis-trifluoromethyl aniline functionalized NDI derivative **10** displayed excellent thermally resistant and high electron mobility of up to 0.24 $cm^2 V^{-1} s^{-1}$ with a negligible decrease in μ_e even when exposed to air for 42 days.[47]

Besides NDIs,[29,30,44–47] the fluorocarbon-based air barrier mechanism[29] was also successfully applied to perylene diimides (PDIs), pyromellitic diimides, and other n-type molecules, affording many ambient-stable n-type OSCs for OTFTs.[48–56] A

series of *N*-fluoro-phenyl functionalized PDI derivatives were studied for n-channel OTFTs by Chen, Bao and their coworkers, their-based OTFTs performed well in air with electron mobilities slightly lower than those measured in glove box, of which the

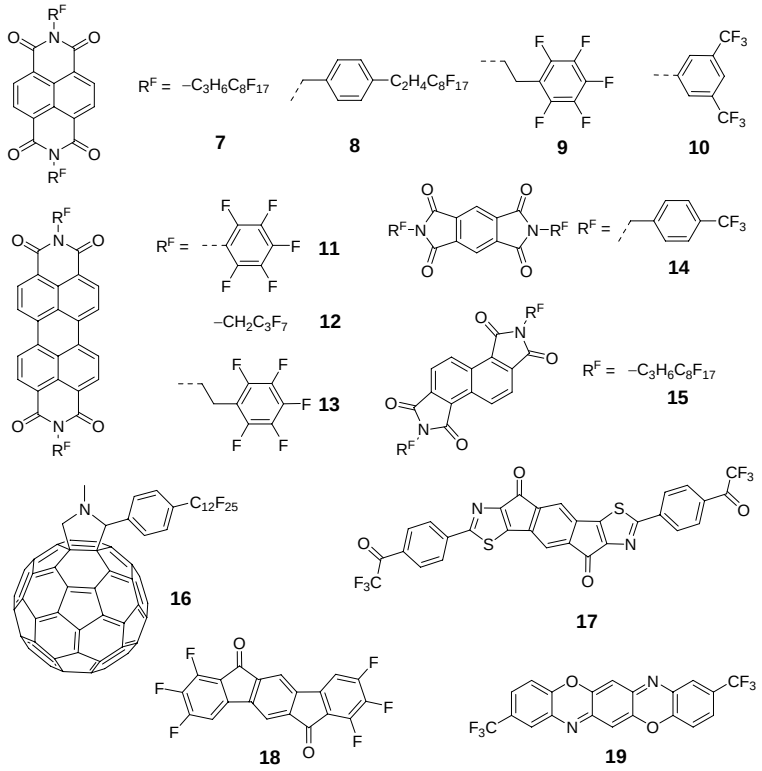

Scheme 2. Representative n-type OSCs designed from a fluorine- or fluorocarbon-based air barrier mechanism

OTFTs based on an *N*-pentafluorobenzene substituted NDI derivative **11** exhibited optimized μ_e values of 0.053 and 0.068 $cm^2\ V^{-1}\ s^{-1}$ in air and in glove box, respectively.[48] More R^F functionalized PDI-based n-type OSCs were developed by Würthner, Bao and their coworkers, and were successfully applied for air-stable n-channel OTFTs.[49] A PDI derivative with two *N*-$CH_2C_3F_7$ groups (**12**) showed the best device performance, with electron mobilities of up to 1.44 and 1.24 $cm^2\ V^{-1}\ s^{-1}$ measured in N_2 atmosphere and in air, respectively ($I_{on/off}$: 10^6).[49] OTFTs based on an *N*-pentafluorophenylethylated PDI derivative (**13**) also exhibited high μ_e values of

0.62 and 0.37 $cm^2 V^{-1} s^{-1}$ tested in N_2 atmosphere and in air, respectively, with $I_{on/off}$ of 10^6–10^7.[49] R^F substituted pyromellitic diimides, such as **14**, were reported by Katz *et al.* for air-stable n-channel OTFTs, these n-type OSCs have the minimal cores but showed relatively high electron mobility of up to 0.079 $cm^2 V^{-1} s^{-1}$ with $I_{on/off}$ as high as 10^6.[50] Zheng and co-workers applied the fluorocarbon-based functionalization on the angular-shaped 1,2,5,6-NDIs and studied their BGTC OTFTs.[51,52] The R^F functionalized 1,2,5,6-NDIs showed better device performance in N_2 atmosphere, with electron mobility of up to 0.52 $cm^2 V^{-1} s^{-1}$ for **15**-based OTFTs, when tested in air, the μ_e values were much lower (about 10^{-2} $cm^2 V^{-1} s^{-1}$).[52] The less air stability of R^F-1,2,5,6-NDIs-based OTFTs is due to the materials' high LUMO energy levels (about –3.6 eV) that could result in electron trapping under ambient conditions,[52] while the corresponding R^F-1,4,5,8-NDIs have relatively lower LUMO energy levels (about –3.9 eV) and better device air stability.[29, 44–47] Fullerene derivatives are a class of n-type OSCs, while most fullerenes could not exhibit n-channel OTFT characteristics in air due to the electron trapping by ambient spices. Perfluoroalkyl-substituted C_{60} derivatives (such as **16**) were developed by Chikamatsu *et al.* and the air operation for their-based n-channel OTFTs was realized, with the electron mobility of up to 0.078 $cm^2 V^{-1} s^{-1}$.[53] Since these perfluoroalkyl-substituted C_{60} derivatives have the high LUMO energies of about –3.6 eV, the fluorocarbon-based air barrier contributes to the device air stability. Compounds **17**–**19** have the electron-deficient π-cores and fluorine or fluorocarbon-based groups with the LUMO energies of –3.79, –3.53 and –3.67 eV, respectively.[54–56] BGTC

OTFTs based on **17**–**19** showed well n-channel FET characteristics, with electron mobilities of up to 0.39, 0.16 and 0.07 $cm^2\ V^{-1}\ s^{-1}$, respectively, and $I_{on/off}$ of 10^5–10^7.[54–56] In spite of the high LUMO energy levels (–3.5 ~ –3.8 eV) of **17**–**19** that go against ambient-stable electron transport,[23–26] their-based OTFTs exhibited good air stability due to the fluorine or fluorocarbon-based air barrier formed by the dense molecular packing.[54–56]

For compounds **7**–**19**, most of their LUMO energy levels are higher than –4.0 eV, the fluorine or fluorocarbon-based air barrier mechanism dominates their n-channel device air stability. In addition, compounds **7**–**19** have relatively large HOMO–LUMO gaps and low-lying HOMO energy levels (–6.0 eV), which blocks the hole transport and makes the unipolar n-channel charge carrier transport. Therefore, the molecular design by using fluorine or fluorocarbon-based air barrier mechanism could afford promising n-type OSCs for ambient-stable, unipolar, n-channel OTFTs. However, most of fluorocarbon-functionalized n-type OSCs suffer from a low solubility in common organic solvents, which hinders their applications for solution-processed OTFTs.

3.2 The functionalization of electron-deficient π-conjugated systems by using electron-withdrawing groups, an energetic mechanism

Compounds **20**–**31** are displayed in Scheme 3 to illustrate the molecular design strategy in this section. The vulnerability of n-type charge carriers is due to the trapping by the most common reactive species in ambient atmosphere (H_2O and O_2). de Leeuw and co-workers first studied the issue of ambient carrier stability in n-type

OSCs and presented a thermodynamically stable model of n-type OSCs' charge carrier transport based on solution-phase electrochemical potentials (*vs* SCE): a reduction potential more positive than –0.658 V is stable towards H_2O and more positive than +0.571 V is stable towards O_2, and an overpotential of about 0.5–1.0 V towards O_2 is required for electrochemical stability of n-type OSCs.[21] In fact, n-type OSCs with first reduction potentials more positive than –0.658 V (*vs* SCE) are common, while it is not practical to find or synthesize electron-deficient molecules with reduction potentials higher than +0.571 V. By studying ambient/operating stability of n-channel OTFTs based on nonfluorinated arylene diimides and other n-type OSCs, Marks and co-workers presented an empirical "energetic mechanism" for air-stable electron transport in n-channel OTFTs: n-type OSCs with first reduction potentials ≥ –0.4 V (*vs* SCE) could operate in air without severe device performance degradation, and the ones with first reduction potentials > –0.1 V (*vs* SCE) could operate well in air with minimal hysteresis and performance degradation.[23–26] That is, the deep LUMO energy levels of n-type OSCs could stabilize the injected charge carriers against the reactions with ambient species (H_2O and O_2) and thermodynamically determine the air/operating stability of n-channel OTFTs. An onset LUMO energy of –4.0 ~ –4.1 eV is essential to stabilize electrons during charge transport,[25] and LUMO level < –4.3 is better for ambient-stable electron transport,[24] but much lower LUMO energies (≤ –4.5 eV) may result in "always on" transistors and low $I_{on/off}$ values due to unintentional doping.[36,57] Therefore, for n-type OSCs, a LUMO energy between –4.1 and –4.4 eV would be desirable for air-stable electron

transport with minimal doping and high $I_{on/off}$ values.

The introduction of two cyano groups onto the core of electron-deficient arylene diimides is an efficient strategy to achieve n-type OSCs with deep LUMO energy levels.[23,24,36,57] PDI-CN2 derivatives **5** and **20** have the LUMO energies of about –4.3

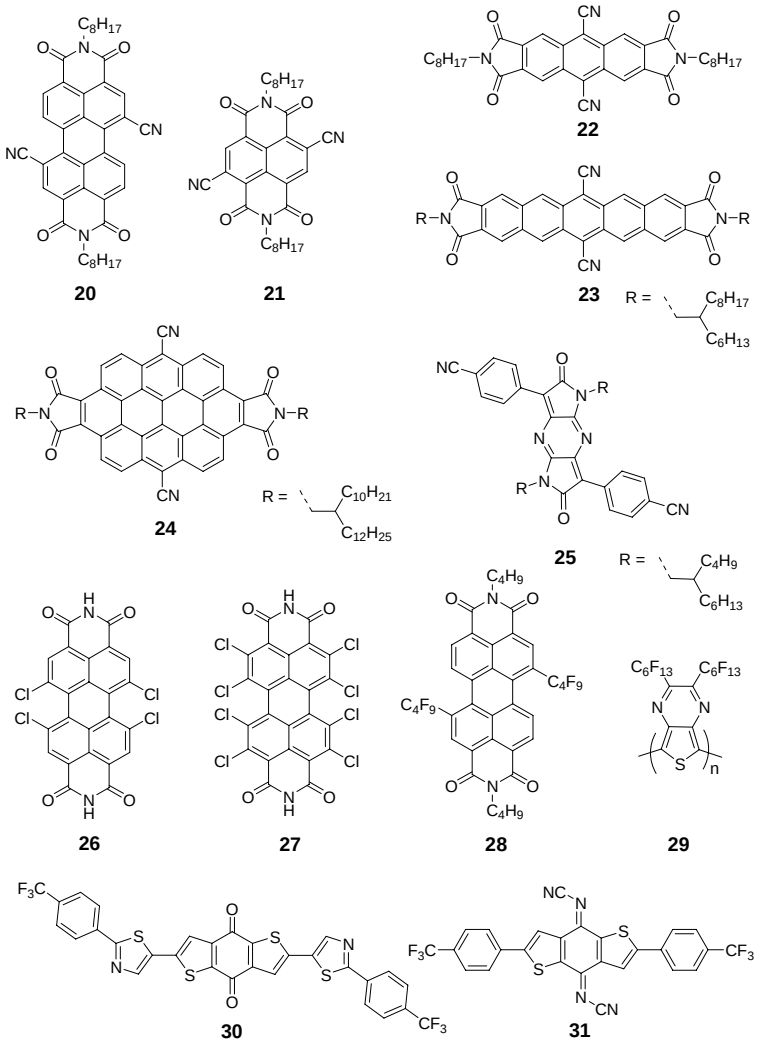

Scheme 3. Representative n-type OSCs designed from an energetic mechanism

eV and their-based vacuum-deposited BGTC OTFTs showed optimized electron mobility of about 0.1 $cm^2 V^{-1} s^{-1}$ in air with excellent ambient/operating stability.[24,36] The solution-processed BGTC or BGBC OTFTs based on **20** exhibit μ_e values of about 10^{-2} $cm^2 V^{-1} s^{-1}$ with $I_{on/off}$ of 10^3–10^5 and V_T values within ±10 V.[58,59] The first

reduction potential (*vs* SCE) of NDI-CN2 derivative **21** is about +0.08 V, demonstrating a very low LUMO energy level of –4.5 eV, which made **21**-based BGTC OTFTs operate well in air with average electron mobility of 0.11 $cm^2 V^{-1} s^{-1}$ and also a relatively lower $I_{on/off}$ value of 10^3 due to unintentional doping.[57] Moreover, dicyano anthracene diimides (ADI), pentacene diimides (PADI) and ovalene diimides (ODI) derivatives **22–24** were synthesized for n-channel OTFTs, their-based BGTC devices could operate in air with electron mobilities of up to 0.02, 0.07 and 0.51 $cm^2 V^{-1} s^{-1}$, respectively.[23,60,61] n-Channel OTFTs based on **22** or **23** measured in air showed comparable device performance to those tested in N_2 atmosphere due to the low-lying LUMO energies of **22** and **23** (–4.1 ~ –4.2 eV).[23,60] ODI-CN2 **24** has a relatively higher LUMO level of –3.9 eV and exhibits a big deviation of device performance from ambient testing (μ_e: 0.51 $cm^2 V^{-1} s^{-1}$) to N_2 atmosphere measurement (μ_e: 1.0 $cm^2 V^{-1} s^{-1}$).[61] Besides arylene diimides derivatives, this cyanation strategy has been applied to other electron-deficient π-systems towards ambient-stable n-type OSCs for OTFTs, such as the recently reported cyano-disubstituted dipyrrolopyrazinedione **25** whose solution-processed TGBC OTFTs showed electron mobility of up to 0.16 $cm^2 V^{-1} s^{-1}$ in air, with $I_{on/off}$ of 10^5–10^6.[62] Tetrachloro PDI derivative **26** reported by Bao and co-workers for vapor-deposited BGTC OTFTs showed well n-channel FET behavior in air with electron mobility on the order of 0.1 $cm^2 V^{-1} s^{-1}$.[31] Four chlorine atoms are not enough to depress the LUMO level of **26** below –4.0 eV, and the relatively higher LUMO energy level of –3.9 eV could not explain the air stability for **26**-based n-channel

OTFTs, where the good thin-film morphology (such as the large grain sizes) was thought as the kinetic factor for device air stability.[31] Octachloro PDI derivative **27** was demonstrated by Würthner, Bao and their coworkers, in comparison with **26**, the doubled core-substituted chlorine atoms make **27** a deep LUMO leveled n-type OSC (LUMO: –4.23 eV).[63] The **27**-based vacuum-deposited BGTC OTFTs showed comparable device performance when measured in N_2 atmosphere and in air, with electron mobilities of up to 0.91 and 0.82 $cm^2 V^{-1} s^{-1}$, respectively, and $I_{on/off}$ of 10^7–10^8.[63] More importantly, these high μ_e values and $I_{on/off}$ ratios were almost unchanged even after exposing the devices to air for about 20 months ($\mu_e \approx 0.60$ $cm^2 V^{-1} s^{-1}$ and $I_{on/off} \approx 10^7$).[63] The high electron mobility and excellent air stability of **27**-based OTFTs are probably due to the energetically low-lying LUMO level and the hydrogen-bond-directed molecular dense brickstone packing.[63] Besides acting as a kinetic air barrier,[29] fluorocarbon-based functional groups could also serve as electron-withdrawing moieties directly attaching on the electron-deficient π-cores to achieve deep LUMO leveled n-type OSCs. n-type OSCs **28**–**31** are the examples for this molecular design with deep LUMO levels of about –4.1 ~ –4.2 eV, their-based OTFTs performed well in air as n-channel transistors although the μ_e values are not high (10^{-6} ~ 0.1 $cm^2 V^{-1} s^{-1}$), where the fluorocarbon-based groups might have the dual functions (kinetic and energetic factors) for realizing device air stability.[64–67]

3.3 The functionalization of electron-deficient π-conjugated systems by using both electron-withdrawing groups and fluorine/fluorocarbon-based functional groups, an energetic/kinetic combined mechanism

PDI derivative **6** (Scheme 1) not only have two electron-withdrawing cyano groups on the perylene core but also bears two fluorocarbon-based *N*-groups at the six-membered imide rings, and an energetic/kinetic combined mechanism could be envisioned for ambient stability of **6**-based n-channel OTFTs. The applications of **6** in high-performance ambient-stable n-channel OTFTs have been described detailedly in section 2. Compounds **32**–**41** (Scheme 4) are representative n-type OSCs designed by using the energetic/kinetic combined mechanism. Beside the lower V_T values, higher μ_e values were found for OTFTs based on ADIF-CN2 (**32**, 0.06/0.04 $cm^2\ V^{-1}\ s^{-1}$ measured in vacuum/air) relative to the devices based on ADI-CN2 (**22**, 0.03/0.02 $cm^2\ V^{-1}\ s^{-1}$) due to the denser molecular packing induced by the R^F side chains and the relatively lower LUMO energy of **32** (–4.2 eV) versus **22** (– 4.07 eV) for easier electron injection.[23,68] Core-fluorinated PDI derivatives bearing R^F *N*-groups **33**–**35** were applied for n-channel OTFTs by Würthner, Bao and their coworkers, while the electronegative fluorine atoms showed limited electron-withdrawing ability and the LUMO energies of **33**–**35** are still higher than –4.0 eV (–3.88 ~ –3.94 eV).[49,69] OTFTs based on **33**–**35** operated well in air with the optimized μ_e values of 0.61, 0.51, and 0.031 $cm^2\ V^{-1}\ s^{-1}$, respectively, and the $I_{on/off}$ ratios of 10^5–10^7,[49,69] the device air stability might be explained by a kinetic dominated and energetic/kinetic combined mechanism. In comparison with the LUMO energy of **35** (–3.93 eV),[69] compound **36** has a lower LUMO energy level value of –4.11 eV,[49] indicating that chlorine atom is more efficient than fluorine atom for withdrawing electron from π-systems as revealed by Bao et al.[70] Wang and coworkers reported a core-perfluoroalkylated and

R^F *N*-functionalized PDI derivative **37** that has the deep LUMO energy level of about –4.2 eV, and **37**-based BGTC OTFTs operated well in air with μ_e, $I_{on/off}$ and V_T values of 0.003 $cm^2\ V^{-1}\ s^{-1}$, 4×10^3 and 4.7 V, respectively.[64]

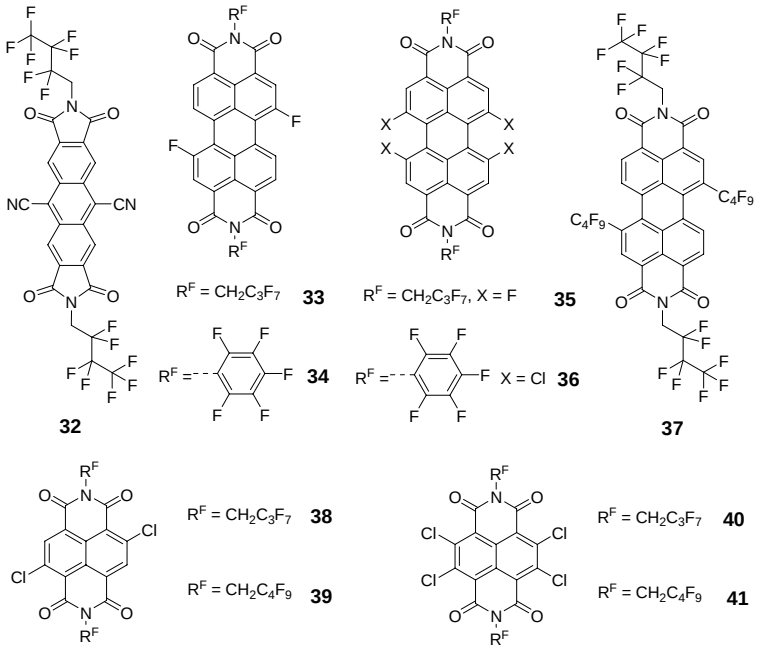

Scheme 4. Representative n-type OSCs designed from an energetic/kinetic combined mechanism

Core-chlorinated and R^F *N*-functionalized NDI derivatives **38**–**41** were developed by Bao, Würthner and their co-workers, and were applied for vacuum-deposited BGTC n-channel OTFTs.[71] The dichloro R^F NDIs **38** and **39** exhibited comparable device performance when measured in N_2 atmosphere and in air, with μ_e values (N_2/air) of 0.86/0.91 and 1.26/1.43 $cm^2\ V^{-1}\ s^{-1}$, respectively, and $I_{on/off}$ of 10^5–10^7.[71] After exposing the devices to air for 3 months, the average mobilities of OTFTs based on **38** and **39** could hold about 80% of the initial values, demonstrating the excellent device ambient stability.[71] In comparison with OTFTs based on **38** and **39**, the devices of tetrachloro R^F NDIs **40** and **41** showed much lower μ_e values (N_2/air) of 0.15/0.021

and 0.44/0.04 $cm^2 V^{-1} s^{-1}$, respectively, with about a ten-fold deviation for the values measured in N_2 and in air.[71] Although **40** and **41** have relative lower LUMO energies (–4.1 eV) than **38** and **39** (–4.0 eV), **40** and **41** have the inferior device performance and air stability than those of **38** and **39**, which should be ascribed to the lower packing density of the fluorinated side chains and the slightly larger π–π stacking distances of **40** and **41** relative to **38** and **39**.[71] Therefore, the unfavorable kinetic factors could explain the poor device air stability of **40** and **41**,[71] their distorted π-cores (versus the nearly planar π-cores of **38** and **39**) might be the internal factors for the inferior device performance and air stability. Würthner and co-workers demonstrated that OTFTs of **38** could be easily processed into large OTFT device arrays with appreciable homogenous performance and μ_e values of up to 0.95 $cm^2 V^{-1} s^{-1}$ in air by solution shearing onto common SiO_2-covered silicon wafers.[72] Recently, SCFETs based on microribbons of **38** were displayed by Würthner *et al*,[73] with the optimized μ_e, V_T and $I_{on/off}$ values of 8.6 $cm^2 V^{-1} s^{-1}$, 9 V and 7×10^7, respectively, and less than 13% degradation in mobility was observed for the microribbon-FET device of **38** in air during a period of 82 days.[73] Single crystal analysis of **38** indicated that the high molecular packing density (20.46 g/cm^3), the close contacts between adjacent π-scaffolds (about 3.27 Å), and the densely packed fluoroalkyl chains with F···F and F···O interactions, which could explain the high device performance and excellent air/operating stability of **38**-based n-channel OTFTs.[73]

3.4 The construction of donor-acceptor (D–A) structures towards high performance n-type OSCs

π-functional materials with donor-acceptor (D–A) structures are common in organic electronics, especially for donors of bulk-heterojunction organic photovoltaic (BHJ OPV) and p-type OSCs for OTFTs due to the intramolecular charge transfer (ICT)-induced low band gap and the strong intermolecular D–A interactions.[74] However, the construction of D–A structure for designing n-type OSCs did not cause wide attention until recently.

3.4.1 n-type D–A copolymers

Polymers **42**–**57** (Scheme 5) are representative n-type OSCs designed by the construction of D–A structure. In 2007, Zhan and coworkers reported a PDI-based D–A polymer (**42**) and applied it as n-type OSC for BGTC OTFTs (measured in N_2, μ_e: 0.013 $cm^2 V^{-1} s^{-1}$, V_T: 4.4 V, and $I_{on/off} > 10^4$) and organic acceptor for all polymer OPVs (a power conversion efficiency (PCE) of 1.5%).[75] This pioneering work promotes the development of rylene diimides-based D–A polymers for n-type OSCs. By using acetylene units as linkers between PDI and dithienothiophene (DTT) segments, Zhan *et al.*[76] prepared a copolymer **43**, the **43**-based BGTC and BGBC OTFTs performed well in air with electron mobility of 0.06 and 0.075 $cm^2 V^{-1} s^{-1}$, respectively. The better air stability and higher electron mobility of OTFTs based on **43** (versus those of **42**) are due to the densely ordered packing of the polymer chains and the lower LUMO energy (–4.0 eV) of **43** versus **42** (–3.9 eV).[75,76] It is interesting that the device performance and stability changed with the device structures, the BGBC devices of **42** and **43** showed higher μ_e values than their BGTC ones, and **42**-based BGBC OTFTs operated well in air with electron mobility of 0.038 $cm^2 V^{-1}$

s^{-1} rather than its air-inactive BGTC devices.[76] To further pursue air stable n-type PDI copolymers, Zhan and co-workers select fluorenone as "acceptor" or "weaker donor" to construct new PDI copolymer **44**, and OTFTs based on **44** performed well in air (μ_e: 0.01 $cm^2\ V^{-1}\ s^{-1}$) thanks to the polymer's low-lying LUMO energy (–4.0 eV).[77] A diethynylbenzene-linked PDI copolymer **45** was recently reported by Marder, Ree and their coworkers, which could form a nanowire suspension in chloroform.[78] **45**-based OTFTs were fabricated by spin-coating its nanowire suspension on OTS-treated SiO_2/Si substrates and could performed in air as n-channel transistors. When annealed at a high temperature (200 °C), the BGTC devices yielded high μ_e and $I_{on/off}$ values of 0.15 $cm^2\ V^{-1}\ s^{-1}$ and 10^6, respectively, with a low threshold voltage (8 V) and negligible hysteresis (0.5 V).[78]

The dithiophene (T2)-linked PDI/NDI D–A polymers **46** and **47** were developed by Facchetti *et al*, their-based BGTC OTFTs measured in vacuum showed electron mobilities of about 0.002 and 0.06 $cm^2\ V^{-1}\ s^{-1}$, respectively, and obvious degradations of device performance were observed for these two polymers due to their relatively higher LUMO energies (> –4.0 eV).[79] However, something amazing happened when P(NDI2OD-T2) **47** was applied for top-gate bottom-contact (TGBC) OTFTs, very high electron mobilities of up to 0.85 $cm^2\ V^{-1}\ s^{-1}$ were achieved under ambient conditions with $I_{on/off}$ of 10^6–10^7, and the TFT stability data tested in ambient conditions were excellent.[80] This excellent device air stability is probably due to the TGBC device structure where the active layer was sandwiched by the dielectric and the substrate. The thiophene-vinylene-thiophene (TVT) building block functionalized

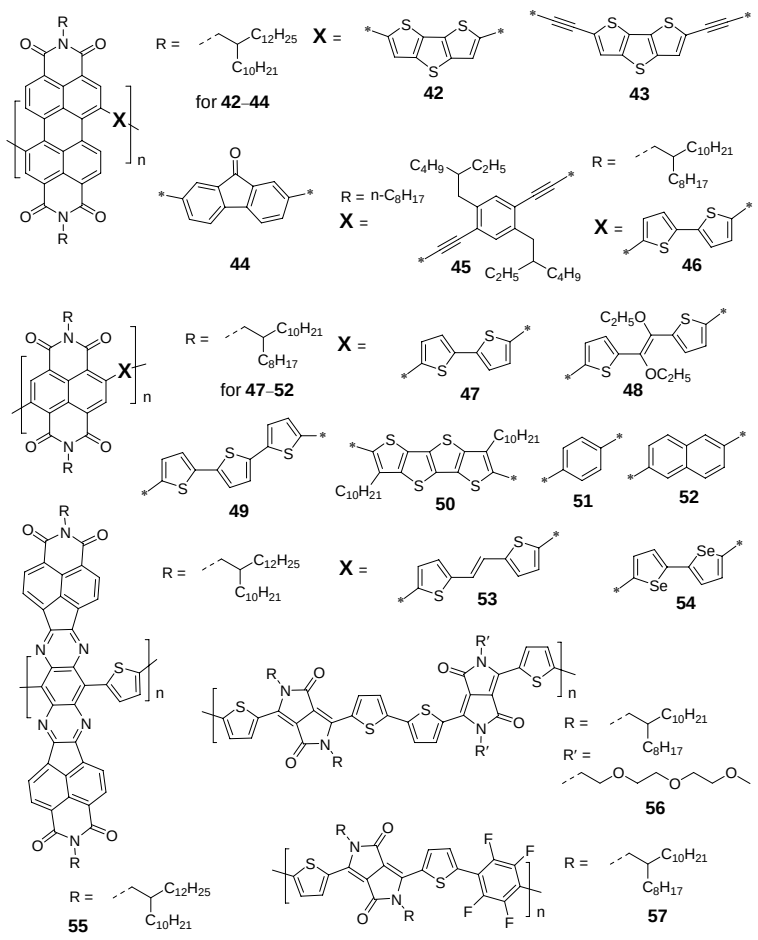

Scheme 5. Donor–acceptor copolymers for n-type OSCs

with alkoxyl groups at the C=C linkage was applied for constructing D–A copolymer **48** by Marks, Facchetti and their co-workers,[81] and **48**-based BGTC and TGBC n-channel OTFTs operated well in air with electron mobilities of up to 0.2 and 0.5 $cm^2 V^{-1} s^{-1}$, respectively, and the low-lying LUMO energy level of **48** (–4.0 eV) could explain its good device stability. By varying the number of thiophene units, Luscombe et al. reported a series of NDI-oligothiophene-based polymers, of which PNDI-3Th (**49**)-based BGTC OTFTs exhibited a maximum electron mobility of 0.076 $cm^2 V^{-1}s^{-1}$ measured in N_2 atmosphere.[82] Later on, some fused-thiophene containing NDI-based copolymers (such as **50**) were developed, their-based OTFTs showed either n-channel or electron-dominated ambipolar charge-transport behaviors, with electron mobilities

of about 10^{-3}–10^{-2} cm^2 $V^{-1}s^{-1}$ measured in N_2 atmosphere.[83,84] Copolymers comprising thiophene-based strong donors and NDI acceptors usually have the low band gaps and relatively high HOMO energies (mostly higher than –5.8 eV), the high HOMO levels make hole transport possible and go against the unipolar n-channel charge transport.[84] When the weaker donors such as benzene and naphthalene were used for constructing NDI-based copolymers (**51** and **52**, with HOMO energies of about –5.9 and –6.1 eV, respectively), the unipolar n-channel charge transport was achieved with electron mobilities of about 10^{-3}–10^{-2} $cm^2\,V^{-1}s^{-1}$ due to the low-lying HOMO energy levels that block the hole transport.[85] Copolymers based on NDI and TVT units were independently studied by Chen, Kim and their coworkers, of which polymer **53**-based TGBC OTFTs showed electron mobility of up to 1.5 $cm^2\,V^{-1}s^{-1}$ or even higher in air due to the low-lying LUMO energy levels (about –3.9 ~ 4.0 eV), the densely packed polymeric backbones, and good thin film morphology.[86,87] Obvious ambipolar charge transport behaviors were observed for all BGTC/BGBC/TGBC OTFTs of these NDI-TVT-based polymers,[86,87] while the unipolar n-channel charge transport could be realized for **53**-based TGBC OTFTs by using Cs_2CO_3-treated source/drain Au electrodes, with electron mobility of up to 1.8 cm^2 $V^{-1}s^{-1}$.[87] A number of selenophene–NDI D–A polymers were developed recently,[85,88,89] and their-based BGTC OTFTs exhibited n-channel or electron-dominated ambipolar charge-transport behaviors, of which devices based on the end-capped polymer **54** showed electron mobility of up to 0.24 $cm^2\,V^{-1}s^{-1}$.[89] This value is much higher than that of P(NDI2OD-T2, **47**)-based BGTC OTFTs (0.06 cm^2

$V^{-1}s^{-1}$).[79]

Recently, Jenekhe et al. reported a thiophene-tetraazabenzodifluoranthene diimide based D–A polymer **55** that comprises a big acceptor unit and a small donor (thiophene) moiety.[90] BGTC OTFTs based on **55** exhibited unipolar n-channel transport with electron mobility of up to 0.30 $cm^2\ V^{-1}s^{-1}$ measured in N_2 atmosphere.[90] In recent years diketopyrrolopyrrole (DPP)-based D-A polymers are mostly developed for high performance p-channel OTFTs, some of which exhibited hole mobilities larger than 10 $cm^2\ V^{-1}s^{-1}$.[6,7] The efforts in developing DPP-based copolymers for n-channel OTFTs are eye-catching, for example, the BGTC OTFTs based on electron-deficient DPP D–A polymers **56** and **57** showed electron mobilities of up to 3 and 2.36 $cm^2\ V^{-1}s^{-1}$, respectively.[91,92] The **57**-base n-channel OTFTs also displayed excellent air stability, with the electron mobility decreasing from 2.36 to 1.88 $cm^2\ V^{-1}s^{-1}$ after a 7-month storage under ambient conditions, the device stability and high electron mobility might be attributed to the polymer's low-lying LUMO energy level of –4.18 eV and the unique edge-on/face-on orientations in thin films.[92] However, even the electron-deficient DPP-based copolymers **56** and **57** still could not completely shut down the hole transport in their OTFTs due to their relatively higher HOMO energy levels (≥ –5.65 eV).[91,92]

3.4.2 n-type small molecules with D–A structures

As mentioned in section 3.2, the functionalization of electron-deficient π-conjugated systems by electron-withdrawing groups could afford n-type OSCs with deep LUMO levels for ambient-stable OTFTs. While the introduction of electron-donating

π-conjugated moieties to the electron-deficient π-backbones is usually thought to be not conducive to obtain ambient-stable n-type OSCs for OTFTs due to the limited changed LUMO energies. Now, this opinion seems to be changing. Usta *et al.* reported a D–A small molecule **58** that has a deep LUMO energy level of –4.32 eV, this value is even slightly lower than that of the parent acceptor backbone (–4.30 eV), and the solution-processed BGTC OTFTs based on **58** exhibited an electron mobility of 0.16 $cm^2 V^{-1}s^{-1}$ and an $I_{on/off}$ ratio of 10^7–10^8, with excellent air stability.[25] Zhang and co-workers introduced the electron-donating sulfur-rich rings to the NDI core and obtained a D–A small molecule **59**.[93] It is surprising that compound **59** has a much lower LUMO energy level (–4.4 eV) than the parent NDI derivative (about –3.8 eV).[93] The solution-processed BGTC OTFTs based on **59** performed well in air as n-channel transistors, with μ_e and $I_{on/off}$ values of 0.05 $cm^2 V^{-1}s^{-1}$ and 10^7, respectively.[93] A thiophene-fused NDI derivative **60** was reported recently by Takimiya *et al.*,[94] its LUMO energy level (–4.0 eV) is just slightly lower than the parent NDI compound (–3.9 eV). The vacuum-deposited BGTC OTFTs of **60** showed electron mobility of about 0.05 $cm^2 V^{-1}s^{-1}$ in vacuum and 0.02 $cm^2 V^{-1}s^{-1}$ in air.[94]

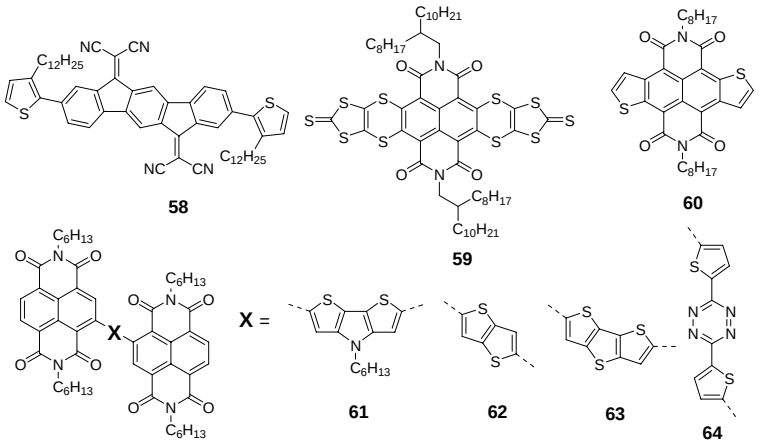

Scheme 6. Donor–acceptor small molecules for n-type OSCs

Marder and coworkers demonstrated that the conjugated donor-bridged bis-NDI derivatives (**61**–**64**) were excellent n-type OSCs for high-performance solution-processed OTFTs.[95,96] The D–A structures make **61**–**64** much higher HOMO energies relative to the parent NDI compound, while their LUMO energy values were almost unchanged versus NDI ($\Delta_{LUMO} \leq 0.12$ eV).[95,96] TGBC OTFTs based on **61** showed electron-dominated ambipolar-transport behaviors with hole and electron mobility of up to 0.0098 and 1.5 $cm^2 V^{-1}s^{-1}$, respectively, the relatively higher HOMO energy of **61** (about −5.4 eV) could explain its hole-transport behavior.[95] TGBC devices based on **62**–**64** exhibited unipolar n-channel transport with electron mobilities > 0.1 $cm^2 V^{-1}s^{-1}$,[95,96] of which **64**-based flexible OTFTs displayed electron mobility of up to 0.17 $cm^2 V^{-1}s^{-1}$ with good air/operating stability.[96]

3.5 Naphthalene diimides fused with sulfur heterocycles and end-capped with electron-withdrawing groups towards high-performance ambient-stable n-type OSCs

The results from sections 3.1–3.4 demonstrate that promising NDI-based n-type OSCs for OTFTs could be designed by the introduction of R^F *N*-substituents, the electron-withdrawing groups, both R^F *N*-substituents and electron-withdrawing groups, or conjugated electron donors to NDI skeleton at imide rings (only for R^F) and/or naphthalene core. In this section, a different molecular design strategy will be introduced by using a series of core-expanded NDIs (c-eNDIs) **65**–**76** (Scheme 7, **71**, **73** and **74** are the mixtures of *cis*/*trans* isomers) that were used in n-channel OTFTs.[97–103] c-eNDIs **65**–**76** were designed and synthesized by Gao and

co-workers,[97–100] the inspiration of molecular design comes from the previous research experiences[104–106] and Yamashita *et al.*'s pioneering work on organic acceptors.[107] The molecular design strategy for these c-eNDIs (such as **65**–**76**) are as follows: (i) the expansion of NDI core by sulfur heterocycles could promote the intermolecular π–π stacking and/or S···S interactions in solid state, which is crucial for achieving high charge mobility; (ii) the end-cap of lateral π-conjugated structure by electron-withdrawing groups (such as C≡N group) can depress molecular LUMO energies, which benefits for the ambient-stable electron injection and conduction; (iii) the long and branched *N*-alkyl chains and the expanded π-conjugation could realize a balance of good solubility, strong and efficient intermolecular interactions in solid state, high crystallinity, and good film formation.[98] c-eNDIs **65**–**76** have good solubility in common organic solvents and low-lying LUMO energy levels of about –4.0 ~ – 4.6 eV.[97–100] The good solubility and deep LUMO energies make these c-eNDIs possible for solution-processed ambient-stable n-channel OTFTs. The solution-processed OTFTs based on **65**–**76** all displayed positive amplification and performed as air-stable n-channel transistors with well-defined linear/saturation regimes, and the μ_e values were in the range of 10^{-3}–3.5 cm^2 $V^{-1}s^{-1}$,[97–103] demonstrating the effectiveness of the molecular design strategy of these c-eNDIs towards solution-processable, ambient-stable n-channel OTFTs. Compounds **65**–**69** are a class of NDI derivatives fused with two 2-(1,3-dithiol-2-ylidene)malononitrile groups (NDI-DTYM2), their-based n-channel OTFTs showed the best device performance among those based on c-eNDIs **65**–**76**. As the excellent n-type OSCs

used in solution-processed OTFTs, NDI-DTYM2 derivatives **65**–**69** will be highlighted in this section.

NDI-DTYM2 derivatives **65**–**68** were designed and synthesized for studying the side-chain influence on their OTFT device performance.[97,98] OTFTs based on **65**–**68** were fabricated by spin coating their respective chloroform solutions on OTS-treated SiO_2/Si substrates (for BGBC and BGTC devices) or poly-(perfluorobutenylvinylether)/glass substrates (for TGBC devices).[102] Compounds **65** and **66** bear the 2-branched $C_{12,8}$ and $C_{10,6}$ *N*-alkyl chains, respectively, with the

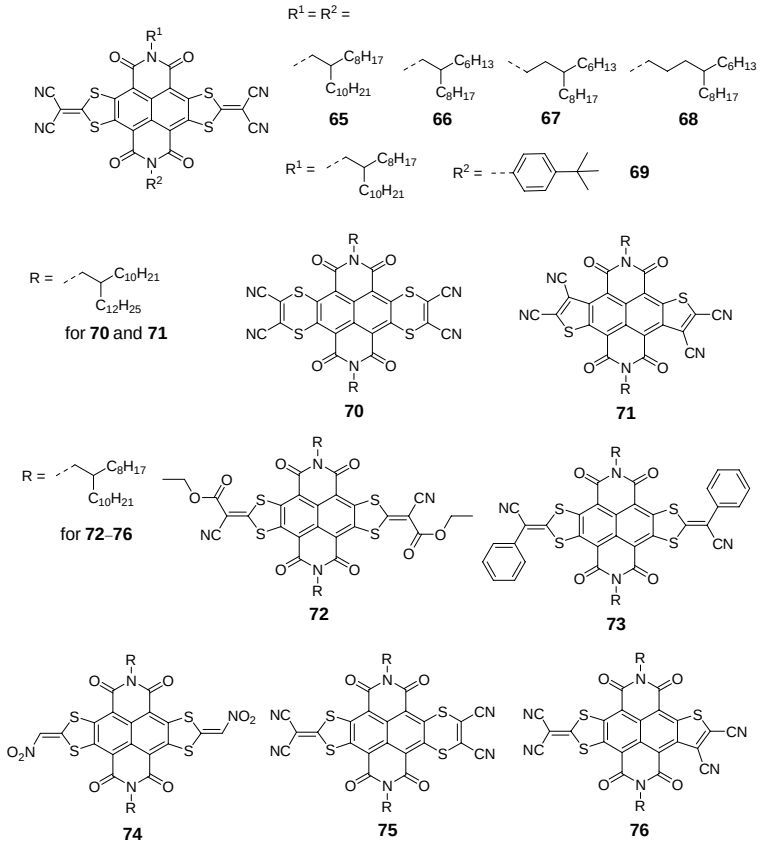

Scheme 7. Core-expanded NDIs for n-type OSCs

deferent side-chain length (carbon atom numbers: 20 *vs* 16). BGTC/BGBC/TGBC OTFTs base on **65** and **66** showed the optimized average electron mobility ($\mu_{e,av}$) of about 0.15–0.5 $cm^2\ V^{-1}s^{-1}$ and 0.08–0.2 $cm^2\ V^{-1}s^{-1}$, respectively, with a 1–2-fold

deviation, demonstrating the limited side-chain influence on device performance.[102] Compounds **66**–**68** have the 2-, 3-, and 4-branched *N*-alkyl chains, respectively, with the comparable chain length (carbon atom numbers: 16–18). The 3-branched compound **67** exhibited the optimized $\mu_{e,av}$ values of 3.0, 2.5, and 0.65 $cm^2 V^{-1}s^{-1}$ for its BGBC, BGTC and TGBC devices, respectively, while OTFTs based on 2-branched compound **66** showed the corresponding mobility values of 0.2, 0.12, and 0.08 $cm^2 V^{-1}s^{-1}$, respectively, leaving a 7–20 times' gap for device performance of **66** and **67**.[102] In addition, OTFTs based on **66** and **67** showed a positive mobility response to the thin-film annealing temperature (even up to 180 °C), while a negative mobility response to the thin-film annealing temperature was found in OTFTs based on 4-branched compound **68**, the μ_e values of **68**-based devices decreased from the as-deposited (or low-temperature annealing ≤ 80 °C) about 0.2 $cm^2 V^{-1}s^{-1}$ to a minimum value of 0.001 $cm^2 V^{-1}s^{-1}$ after annealing at a temperature > 100 °C.[102] The results indicate that the branch-point position of side *N*-alkyl chains significantly affects the device performance of NDI-DTYM2 derivatives.[102] This finding together with Pei and co-workers' work on alkyl chain branching p-type polymers[108] demonstrate that besides the popular work on new π-backbones, the variation of alkyl chain branching point of known or new π-systems is a powerful strategy for achieving high charge carrier mobility through fine tuning molecular packing in solid state. A versatile one-pot synthesis of NDI-DTYM2 derivatives was developed in our lab, which afforded an unsymmetrically *N*-substituted NDI-DTYM2 derivative **69**.[99] The solution-processed BGTC OTFTs based on **69** showed electron mobility as high as

0.7 $cm^2 V^{-1}s^{-1}$ in air, demonstrating that both the symmetrically and unsymmetrically *N*-substituted NDI-DTYM2 are promising n-type OSCs for OTFTs.[99] Moreover, unsymmetrically *N*-substituted **69** has been successfully used in ultra-thin-film (≤ 10 nm) n-channel OTFTs[103] and n-channel thin-film phototransistors.[109] In a word, the high electron mobility (0.1–3.5 $cm^2 V^{-1}s^{-1}$), high current on/off ratios (10^5–10^8), low threshold voltages (< 15 V), as well as the excellent air/operating device stability make NDI-DTYM2 derivatives (such as **65**–**69**) a class of the most promising n-type OSCs for OTFTs.[97–99,101–103] Besides c-eNDIs **65**–**76** mentioned above, some new c-eNDIs bearing the symmetrical or unsymmetrical π-rings on the naphthalene core were developed by Zhang's group and applied in solution-processed, ambient-stable, n-channel OTFTs, with the electron mobility ranging from 10^{-3} to 0.22 $cm^2 V^{-1}s^{-1}$.[110–112]

3.6 Quinoidal thiophene derivatives terminated with cyano-containing methylenes towards high-performance ambient-stable n-type OSCs

7,7,8,8-tetracyanoquinodimethane (TCNQ) is a typical n-type OSC with low-lying LUMO energy level of about –4.8 eV. In 1994, Brown and co-workers reported OTFTs based on TCNQ, while the electron mobility is very low (about 10^{-5} $cm^2 V^{-1}s^{-1}$) as well as the low $I_{on/off}$ values.[113] Later on, Uemura *et al.*[114] prepared the air-stable n-channel single-crystal transistors based on TCNQ, the devices showed high μ_e values of up to 0.5 $cm^2 V^{-1}s^{-1}$ with negligible threshold gate voltages, demonstrating the great potential of quinoidal derivatives in n-channel OTFTs.

As shown in Scheme 8, quinoidal thiophene derivatives terminated with

cyano-containing methylene are becoming a class of promising n-type OSCs for OTFTs.[115–123] A dicyanomethylene-terminated quinoidal terthiophene derivative **77** was first applied in n-channel OTFTs by Pappenfus *et al*.,[115] electron mobilities of

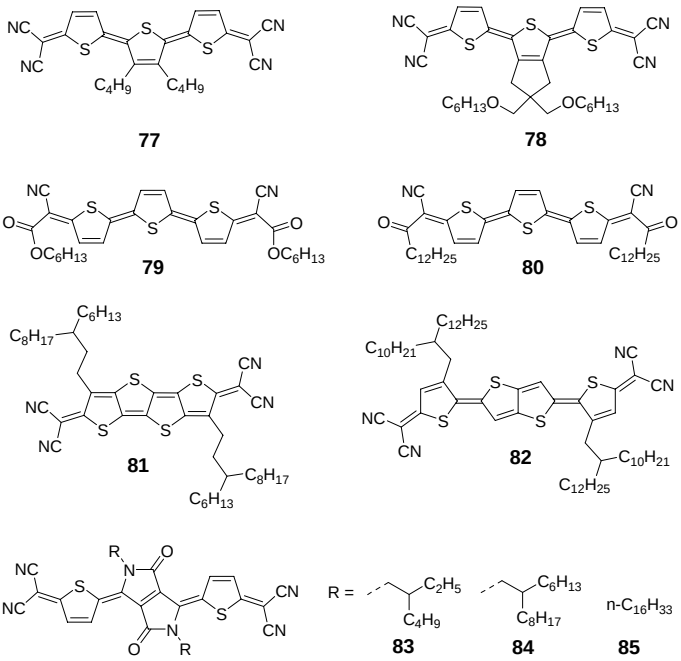

Scheme 8. Quinoidal thiophene derivatives terminated with cyano-containing methylenes for n-type OSCs

about 10^{-3} cm^2 $V^{-1}s^{-1}$ were achieved for both vacuum-deposited and solution-processed BGTC (Ag source/drain contacts) devices.[115] A much higher μ_e value of about 0.2 $cm^2 V^{-1}s^{-1}$ and a high $I_{on/off}$ ratio of 10^6 were realized in **77**-based vacuum-deposited BGBC (Au source/drain contacts) OTFTs, where the substrates were held at 130 °C during the deposition of thin film of **77** and the devices were measured in high vacuum due to the device air sensitiveness.[116] A series of cyano-containing methylene-terminated quinoidal thiophene derivatives such as **78**–**80** were developed by Takimiya *et al*. and applied in n-channel OTFTs.[117–119] The solution-processed BGTC OTFTs based on **78**–**80** all displayed ambient-stable

n-channel FET behaviors with electron mobilities of up to 0.16, 0.015, and 0.06 $cm^2 V^{-1}s^{-1}$, respectively, and the low-lying LUMO energy levels of **78**–**80** (about –4.2 eV) could explain their device air stability.[117–119] Li and co-workers reported a dicyanomethylene-substituted fused tetrathienoquinoid derivative **81** and applied it in solution-processed n-channel OTFTs.[120] In comparison with OTFTs based on dicyanomethylene-end-capped quinoidal oligothiophenes (such as **77**–**80**), **81**-based OTFTs exhibited a much higher electron mobility of about 0.9 $cm^2 V^{-1}s^{-1}$ with good air/operating stability.[120] A number of dicyanomethylene-substituted 2,5-di(thiophen-2yl)thieno-[3,2-b]thienoquinoid derivatives with different alkyl chain positions on the π-backbone were reported by in Li *et al.*,[121] of which the 3,3′-alkylated compound **82** showed the best OTFT performance, with the electron mobility of up to 0.22 $cm^2 V^{-1}s^{-1}$ and $I_{on/off}$ ratios of 10^4–10^5 measured in air, indicating that the alkyl chain location has significant influence on device performance. Compounds **81** and **82** have the comparable LUMO energy levels of about –4.3 eV, which contributes to the device air stability of their-based n-channel OTFTs.[120,121] Recently, diketopyrrolopyrrole(DPP)-containing dicyanomethylene-terminated quinoidal thiophene derivatives **83** and **84** were developed in Zhu's lab,[122] their-based BGTC OTFTs showed ambient-stable n-channel FET behaviors, with electron mobilities of up to 0.55 (vacuum-deposited device) and 0.35 $cm^2 V^{-1}s^{-1}$ (solution-processed device), respectively, as well as high $I_{on/off}$ ratios (10^5–10^6) and excellent air/operating device stability. Compounds **83** and **84** are the first examples for DPP-based OSCs with unipolar electron-transport

characteristics in FET devices. Compound **85**, with the same π-backbone of **83** and **84** but different side chains, was reported by Heeney and coworkers for small-molecule/polymer blended n-channel OTFTs,[123] high electron mobilities of 0.5 $cm^2 V^{-1}s^{-1}$ and $I_{on/off}$ ratios of 10^2–10^3 were achieved for **85**-based TGBC devices. The deep LUMO energy levels of **83**–**85** (about −4.2 ~ −4.5 eV) might explain their excellent device stability in ambient and operating conditions.[122,123]

3.7 Ladder-type small molecules and polymers synthesized by condensation reactions for n-type OSCs

As shown in Scheme 9, ladder-type polymers (**86** and **87**) and small molecules (**88**–**96**) are typical n-type OSCs for OTFTs, which could be readily synthesized by condensation reactions. Poly(benzobisimidazobenzophenanthroline) (BBL, **86**), a

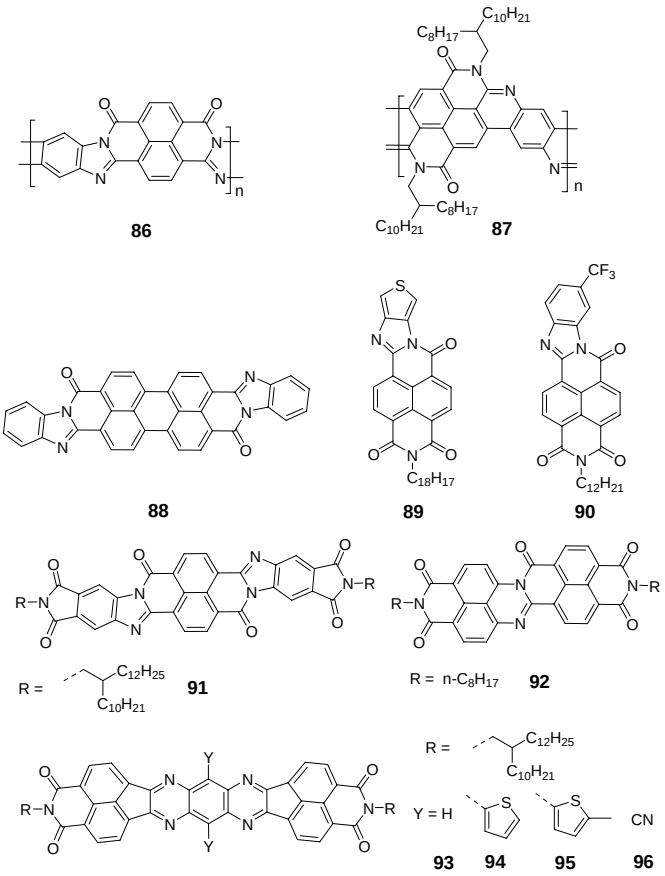

Scheme 9. Ladder-type small molecules and polymers for n-type OSCs

conjugated ladder polymer, was the first class of n-type polymers used for OTFTs, its BGBC OTFTs spin coated from methanesulfonic acid solution showed electron mobility of up to 0.1 $cm^2 V^{-1}s^{-1}$.[124] More importantly, **86**-based n-channel OTFTs exhibited long-term ambient stability over 4 years with negligible changes for μ_e, $I_{on/off}$ and V_T values.[125] The long-term device air stability could be explained by the energetic and kinetic factors, i.e. the deep LUMO energy level of **86** (about 4.0–4.2 eV) and its high crystalline films with the densely packed polymeric chains (about 3.4 Å).[125] A ladder-type polymer **87** was recently reported by Luscombe and coworkers, its spin-coated BGTC OTFTs showed electron mobility as high as 0.0026 $cm^2 V^{-1}s^{-1}$ that was measured in an inert atmosphere due to the high LUMO energy of **87** (–3.54 eV).[126] 3,4,9,10-perylenetetracarboxylic bis-benzimidazole (PTCBI, **88**) was an old n-type OSC that was used in early-stage photovoltaic cells by Tang.[127] Dhagat *et al.* reported the vacuum-deposited BGTC OTFTs based on **88**, giving electron mobility of up to 0.05 $cm^2 V^{-1}s^{-1}$ in N_2 atmosphere.[128] Compounds **89**[129] and **90**[130] are the almost smallest NDI-based ladder-type molecules, but their-based vacuum-deposited BGTC OTFTs showed electron mobilities of up to 0.35 and 0.10 $cm^2 V^{-1}s^{-1}$ (measured in vacuum but with somewhat air stability), respectively, demonstrating their great potential in n-channel OTFTs. Ladder molecules **91**[131] and **92**[132], bearing larger π-systems than **89** and **90**, were recently reported for n-channel BGTC OTFTs, and showed comparable electron mobility of about 0.05 $cm^2 V^{-1}s^{-1}$, **91**-based devices exhibited excellent air and operating stability due to the low-lying LUMO energy

level of **91** (–4.2 eV).[131] A series of tetraazabenzodifluoranthene diimide (BFI) derivatives **93**–**96** (LUMO levels: –3.6, –3.7, –3.5 and –4.3 eV, respectively) were developed by Jenekhe *et al*.,[133] which share a large rigid ladder-type π-backbone and were applied for solution-processed n-channel OTFTs. Bottom-gate devices based on **93**–**96** were measured in N_2 atmosphere and showed electron mobilities of up to 0.03, 0.12, 0.05, and 0.021 $cm^2 V^{-1}s^{-1}$, respectively.[133]

3.8 The construction of acceptor–acceptor (A–A) or acceptor–linker–acceptor (A–L–A) structures for high performance n-type OSCs

As discussed in section 3.4, the construction of donor–acceptor (D–A) structures could afford excellent n-type OSCs for OTFTs, while most n-type OSCs with D–A structures usually have low band gaps and high HOMO energies that make hole transport possible.[84–87,89,91,92] To achieve pure electron-transporting OSCs, the construction of acceptor–acceptor (A–A) and acceptor–linker–acceptor (A–L–A) structures for n-type OSCs is highly desirable. Scheme 10 presents the representative n-type OSCs (**97**–**110**) for OTFTs with A–A or A–L–A structures, the linkers (L) are double bond (**104**), triple bond (**105**), benzene ring (**51** and **106**), or fused benzene ring (**107–110**). These linkers could be regarded as weaker donors relative to the common electron-donating thiophene and its derivatives. Polymer **97** (BBB) was the early A–A polymer used for n-channel OTFTs, its BGBC devices exhibited a very low electron mobility of about 10^{-6} $cm^2 V^{-1}s^{-1}$.[124] Luscombe and co-workers prepared the NDI-based A–A polymers **98**[126] and **99**[82] that have the HOMO/LUMO energies of –3.54/–5.90 and –3.76/–6.50 eV, respectively. The deep HOMO energy levels of **98**

and **99** resist the hole transport and make their-based OTFTs pure n-channel transport. The BGTC OTFTs based on **98** and **99** measured in N_2 atmosphere showed low electron mobilities of about 4×10^{-7} and 6×10^{-4} $cm^2 V^{-1}s^{-1}$, respectively.[82,126] NDI A–A oligomers **100** and **101** with LUMO levels of about −3.8 eV and HOMO energies < −6.5 eV were synthesized by Marder and coworkers,[134] their-based solution-processed TGBC OTFTs showed electron mobilities of up to 0.34 and 0.014 $cm^2 V^{-1}s^{-1}$, respectively. A–A polymers **102**[135,137] and **103**[25] were prepared by Marks *et al*. and were applied for n-channel OTFTs. BGTC devices based on **102** showed molecular weight-dependent mobility, the high and low-molecular-weight **102** samples afforded the different μ_e values of about 0.038 and 0.011 $cm^2 V^{-1}s^{-1}$, respectively, and TGBC OTFTs based on high-molecular-weight **102** exhibited electron mobility of up to 0.189 $cm^2 V^{-1}s^{-1}$.[136] In comparison with devices of **102**, **103**-based BGTC OTFTs showed a much lower μ_e value of about 0.5×10^{-4} $cm^2 V^{-1}s^{-1}$ in N_2 atmosphere.[25]

Recently, Pei and coworkers designed and synthesized an electron-deficient PPV-like polymer **104**,[137] which possesses the A–L–A structure feature, with benzodifurandione-based oligo(*p*-phenylene vinylene) (BDOPV) as the acceptor (A) and double bond as the linker (L). TGBC OTFTs based on **104** displayed high electron mobility of up to 1.1 $cm^2 V^{-1}s^{-1}$ under ambient conditions, the low-lying HOMO/LUMO energy levels of **104** (–6.12/–4.10 eV) contribute to its pure ambient-stable electron transport.[137] In comparison with the TGBC devices, **104**-based BGTC OTFTs exhibited 10-fold-lower electron mobility of about 0.1 cm^2

$V^{-1}s^{-1}$ in air.[137] As a whole, this electron-deficient PPV derivative (**104**) showed comparable or even better device performance (in mobility) relative to the

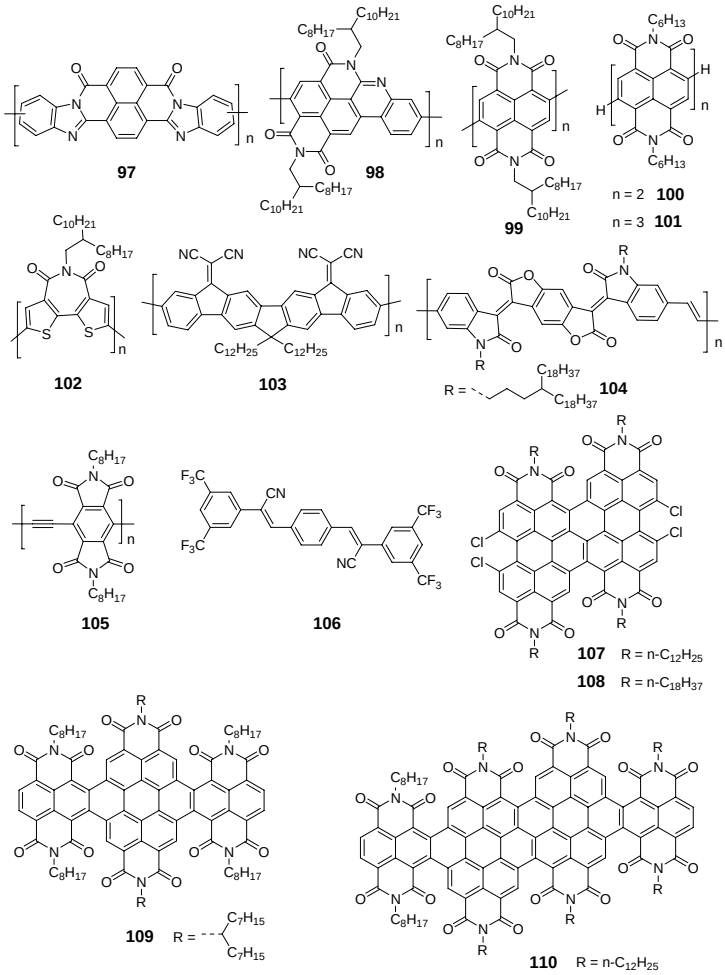

Scheme 10. n-Type OSCs with acceptor–acceptor or acceptor–linker–acceptor structures

well-studied n-channel polymer P(NDI2OD-T2) (**46**).[79,80] A pyromellitic diimide–ethynylene-based A–L–A polymer **105** with HOMO/LUMO energies of about –6.41/–3.84 eV was recently reported by Katz *et al.*,[138] its TGBC OTFTs exhibited unipolar charge transport with electron mobility of about 2×10^{-4} cm^2 $V^{-1}s^{-1}$, making this class of simplest n-channel polymers great potential in organic electronics. Compound **106** containing A–L–A structure feature with benzene as the

linker, is a typical n-type OSC due to its low-lying HOMO/LUMO levels (–6.98/–4.14 eV).[139] **106**-based SCFETs and vacuum-deposited OTFTs showed electron mobilities of up to 0.55 and 0.34 $cm^2 V^{-1}s^{-1}$, respectively, demonstrating the excellent pure electron-transporting property.[139] The fused bis-PDI derivatives **107** and **108**, and the NDI/PDI mix-fused derivatives **109** and **110** were developed by Wang and coworkers,[140–143] these compounds also have the A–L–A structure features where the linkers could be regarded as the fused benzene rings. Compound **107** with the n-$C_{12}H_{25}$ side chains has the low-lying HOMO/LUMO energy levels (–6.04/–4.22 eV), its single-crystal FETs showed high electron mobility of up to 4.65 $cm^2 V^{-1}s^{-1}$ in air,[140] which is much higher than the mobility of the corresponding solution-processed thin-film devices (about 0.14 $cm^2 V^{-1}s^{-1}$ measured in air).[141] Compound **108** shares the same π-backbone with **107** but has the different *N*-alkyl chains. The solution-processed BGTC OTFTs based on **108** that bears the n-$C_{18}H_{37}$ chains exhibited electron mobility as high as 0.7 $cm^2 V^{-1}s^{-1}$ and a high current on/off ratio of 4×10^7 with excellent device ambient stability.[141] The NDI/PDI mix-fused derivatives **109**[142] and **110**[143] have the enlarged π-systems and deep HOMO/LUMO energy levels of –6.16/–4.26 and –6.08/–4.40 eV, respectively, which makes **109** and **110** promising n-type OSCs for transistors. The solution-processed BGTC OTFTs based on **109** and **110** operated well in air with electron mobilities of up to 0.25 and 0.18 $cm^2 V^{-1}s^{-1}$, respectively ($I_{on/off}$: 10^5–10^7).[142,143]

3.9 Electron-deficient metal complexes for potential n-type OSCs

Electron-deficient metal complexes are a class of potential n-type OSCs for transistors

(Scheme 11, **111**–**116**), although they are less studied relative to the common small molecular and polymeric n-type OSCs discussed above. As mentioned in section 2, copper hexadecafluorophthalocyanine (F_{16}CuPc, **1**) is an excellent n-type OSC for ambient-stable n-channel OTFTs.[28] Yan and coworkers reported two tin (IV)-Pc-based n-type OSCs $SnCl_2$Pc (**111**)[144] and SnOPc (**112**)[145] with the LUMO energy levels < –4.0 eV and applied them to vacuum-deposited n-channel OTFTs. The BGTC devices based on **111** and **112**, with the modified substrates by a thin film of *para*-sexiphenyl (< 10 nm), showed electron mobilities of up to 0.44 and 0.3 $cm^2 V^{-1}s^{-1}$, respectively, with good device air stability.[144,145]

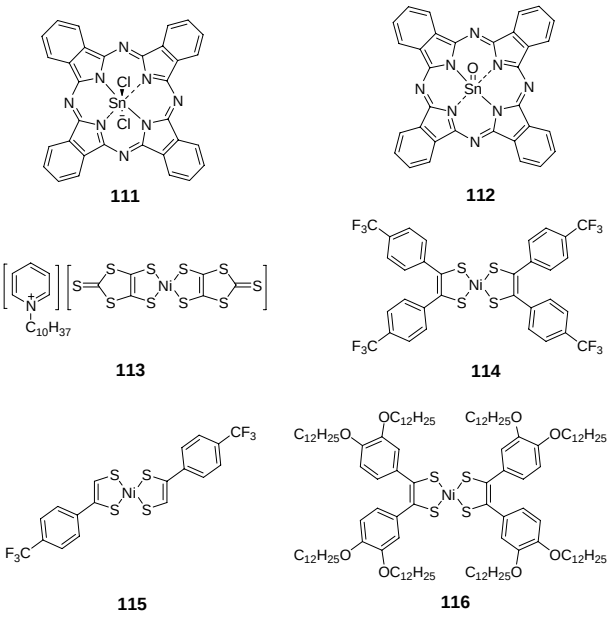

Scheme 11. Electron-deficient metal complexes for n-type OSCs

In 1993, a nickel-$(dimt)_2$ complex **113** was applied to n-channel OTFTs by using Langmuir-Blodgett technique, affording an electron mobility as high as 0.2 $cm^2 V^{-1}s^{-1}$.[146] Later on, some nickel bis(dithiolene) complexes such as **114**–**116** were developed for n-type OSCs used in transistors.[147–149] Mori and coworkers synthesized a number of tetraphenyl nickel bis(dithiolene) complexes (such as **114**) and applied

them to n-channel OTFTs, some of which could performed in air as n-channel transistors but the μ_e (about 10^{-6}–10^{-5} $cm^2 V^{-1}s^{-1}$) and $I_{on/off}$ ($\leq 10^2$) values were very low.[147] In comparison with **114**, a simpler complex **115** was developed by Qin and coworkers, **115**-based vacuum-deposited BGTC OTFTs showed an electron mobility of 0.11 $cm^2 V^{-1}s^{-1}$ and $I_{on/off}$ of 2×10^6, with good device air stability.[148] The solution-processed BGTC OTFTs based on a tetraphenyl nickel bis(dithiolene) complex **116** were studied by Cho *et al.*,[149] affording an electron mobility of 1.3×10^{-3} $cm^2 V^{-1}s^{-1}$ with V_T and $I_{on/off}$ values of 4.6 V and 10^5, respectively. Neutral complexes **114**–**116** have the low-lying LUMO energy levels of about −4.1 ~ −4.6 eV due to the electron-deficient tetravalent Ni ion, which contributes to the device air stability.[147,148] Phthalocyanine metal complexes and the metal dithiolene complexes have been well studied for organic conductors,[150–152] their uses for OSCs especially for n-type ones should draw more attention.

3.10 Other molecular design for n-type OSCs

Besides the strategies mentioned above, there are some molecular systems designed for n-type OSCs. As shown in Scheme 12, the electron-deficient pentacene-like small molecules[153–156] and the side-chain polymers with pendant PDI units[158,159] are two classes of n-type OSCs for OTFTs. A series of π-deficient pentacenequinones were developed by Miao and coworkers.[153] It was found that replacing H atoms of pentacenequinone with F atoms or replacing C atoms with N atoms (**117**) could lower the LUMO energy level of pentacenequinone to yield n-type OSCs with electron mobilities higher than 0.1 $cm^2 V^{-1}s^{-1}$ (measured in vacuum). Vacuum-deposited

OTFTs based on silylethynylated *N*-heteropentacene **118** showed μ_e values in the

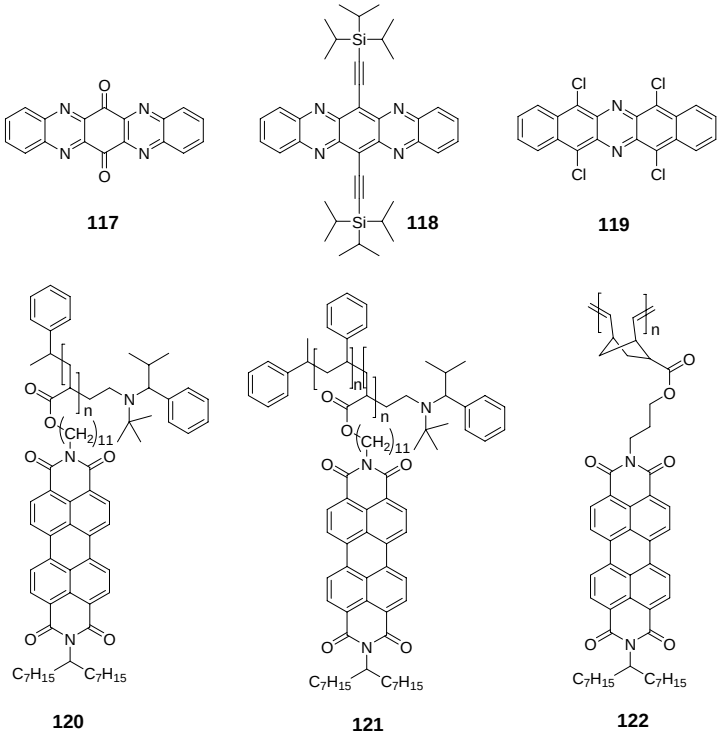

Scheme 12. Electron-deficient pentacene-like derivatives and side-chain polymers with pendant PDI units for n-type OSCs

range of 1.0–3.3 $cm^2 V^{-1}s^{-1}$ (in vacuum), when the devices were tested in air, the μ_e values decreased to 0.3–0.5 $cm^2 V^{-1}s^{-1}$.[154] High-surface-energy self-assembled monolayers (SAMs) of phosphonic acids with oxygen-containing long alkyl chains have been applied for solution-processed n-channel OTFTs of **118** by Miao *et al.*, leading to a high electron mobility of up to 2.5 $cm^2 V^{-1}s^{-1}$ and an on/off ratio of 6×10^5 when tested in vacuum.[155] It is worth noting that single-crystal FETs based on 5,7,12,14-tetrachloro-6,13-diazapentacene (**119**) exhibited a very high electron mobility of 3.39 $cm^2 V^{-1}s^{-1}$ when measured in ambient, although the LUMO energy of **119** is relative high (–3.79 eV).[156] Overall, n-channel OTFTs based on electron-deficient pentacene-like derivatives exhibited unsatisfied device air stability

due to the relative higher LUMO energy levels (≥ −4.0 eV), more electron-deficient pentacene-based n-type OSCs would be the next focus. As shown in Scheme 12, side-chain polymers with pendant PDI units (**120**–**122**) were designed for n-channel OTFTs by Thelakkat, Marder and their respective coworkers,[157–159] with electron mobility of up to 1.2 × 10^{-3} cm^2 $V^{-1}s^{-1}$ (measured in inert gas).[158] The side-chain polymers with pendant π-deficient building blocks (such as PDI, NDI or core-modified PDI/NDI) would attract more attention for their uses in n-channel OTFTs and OPVs (as organic acceptors).

4. Synthesis of n-type OSCs

Synthesis is crucial for developing n-type OSCs and directly determines the cost of the materials. Herein, we choose to highlight some important synthetic strategies for n-type OSCs mentioned above. Aromatic diimides with fluororcarbon-based *N*-groups (**2**, **6**–**15**, and **33**–**41**) are a class of important n-type OSCs for OTFTs and could be prepared by the imidization reactions from commercially available or core-modified bisanhydrides and fluororcarbon-based primary amines. These imidization reactions are typically carried out at elevated temperature in high boiling solvents such as propionic acid, DMF, NMP, quinoline or imidazole, the catalysts (such as zinc acetate dehydrate and acetic acid) are usually used for amines with steric hindrance and electron deficient.[24,29,49,160] Compounds **5**, **6**, **20**–**25** and **32** are air-operable n-channel materials due to the core-attached cyano groups that deep the LUMO energy to a suitable level. The core-cyanations were achieved by the Pd-catalyzed reaction of the dibromo precursor of **5**, **6**, **23** or **24** with $Zn(CN)_2$ or CuCN in the hot dioxane

solution ($Pd_2(dba)_3$·dppf as the catalyst),[36,60,61,161] or by the uncatalyzed reaction of the dibromo precursor of **20–22**, **25**, **32** or **96** with CuCN in the refluxing DMF solvent.[24,57,62,68,133] It should be noting that Diels-Alder reactions are usually used for synthesizing the five-membered-ring acene diimides, such as **22–24** and **32**.[60,61,68] Compounds **33**–**36** were obtained by the Halex reactions of the corresponding dibromo or tetrachloro PDIs with potassium fluoride in sulfolane and in the presence of 18-crown-6 or *N*,*N*′-dimethylimidazolidino-tetramethylguanidinium (CNC^+) fluoride as catalyst.[49] Octachloro PDI **27** and tetrachloro NDIs **40** and **41** were synthesized by the electrophilic reactions of the corresponding core-unsubstituted PDI and NDIs with chlorine in chlorosulfonic acid at 80–85 °C (iodine as catalyst).[63,71] Perfluoroalkylation via copper coupling reactions of dibromo PDIs with perfluoroalkyl iodides in DMSO gave excellent yields of core-perfluoroalkylated PDIs **28** and **37**.[64]

The aryl-aryl coupling reactions are widely used for synthesizing OSCs, of which the Stille coupling reaction is the most usual method for synthesizing π-functional materials.[162] D–A polymers **42**, **46**–**50**, **53**–**55**, **57** and A–L–A polymers **104** and **105** were all prepared by the Stille coupling reactions, where the Pd-catalysts are usually $Pd(PPh_3)_4$ (sometimes with CuI),[75,138] $Pd(PPh_3)_2Cl_2$,[79,80] or $Pd_2(dba)_3$ with $P(o\text{-tolyl})_3$ ligand (commonly used),[81–89] the solvents are anhydrous toluene (commonly used), chlorobenzene, THF, DMF or the mixed solvents, and the reaction temperatures are usually among 80–130 °C depended on the reaction solvents. In addition, the Stille coupling reactions were applied for the syntheses of **17**, **29**, **30**, **58**, **61**–**64**, **87**, **94**, **95**,

98, **100**, **101**, **109** and **110**.[25,65,66,95,96,126,133,134,142,143] The Suzuki-Miyaura coupling reactions were used for synthesizing **31**, **44**, **51**, **52** and **56**, the $Pd(PPh_3)_4$ was commonly used as catalyst with K_2CO_3 or other basic salt in toluene,[67,77,85] of which $Pd_2(dba)_3$, P(o-tolyl)$_3$ ligand, K_3PO_4 and toluene (as solvent) were applied for synthesizing copolymer **56**.[91] Copolymers **43** and **45** containing triple bonds were prepared by the Sonogashira coupling reactions with CuI, Et_3N, and Pd-catalyst $Pd(PPh_3)_4$ or $Pd(PPh_3)_2Cl_2$ in toluene or THF solvent.[76,78] In addition, the Sonogashira coupling reaction was also used for synthesizing compound **60**.[94] Yamamoto polycondensations were successfully utilized for preparing A–A polymers **99**, **102** and **103**, with $Ni(COD)_2$ (catalyst), COD and 2,2′-bipyridyl (ligands) in toluene, DMF or their mixed solvent.[25,82,135] The fused bis-PDIs **107** and **108** were synthesized by the home-coupling reactions of tetrachloro PDIs with CuI as the catalyst, L-proline as the ligand, and K_2CO_3 as the base in DMSO, which involves the traditional Ullmann coupling reaction and C–H transformation with relative lower yields (< 20%).[140,141] The NDI-PDI hybrid rylene arrays **109** and **110** were prepared by the cross-coupling reactions between tetrachloro PDI and monostannyl NDIs, the synthesis undergoes the Stille coupling reaction and C–H transformation using $Pd(PPh_3)_4$ and CuI as catalysts in toluene, giving the moderate yields of 20–46%.[142,143]

The nucleophilic aromatic substitution (S_NAr) reactions were successfully used for preparing c-eNDIs **59** and **65**–**76**, the S_NAr reactions are very simple with 2,3,6,7-tetrabromonaphthalene diimides (TBNDIs) and dithiolate salts reacting in polar solvents such as THF and DMF. Gao and coworkers developed the synthetic

methods for TBNIDs by using a dehydrohalogenation-based imidization reaction.[106,163] Now, TBNDIs have become the key precursors for preparing c-eNDIs.[93,97,98,100,111,112,164–167] It should be noting that NDI-DTYM2 derivatives **65**–**69** could be achieved by a mild one-pot synthesis from 2,3,6,7-tetrabromonaphthalene dianhydride, sodium 1,1-dicyanoethene-2,2-dithiolate, and primary amines in DMF, this one-pot synthesis undergoes a S_NAr reaction and then an imidization reaction, allowing an easy and low-cost access to diverse n-type OSCs.[99]

The quinoidal thiophene derivatives **77**–**85** were usually prepared by a Pd-catalyzed (such as $Pd(PPh_3)_4$) Takahashi coupling reaction from the corresponding dibromo precursor and the cyano-methylene derivative, with the base (e.g. NaH) in organic solvents (e.g. THF and DME), followed by an oxidation reaction with Br_2, air or other oxidants.[117–123] The condensation reactions were utilized in the syntheses of n-type OSCs **86**–**93**, **97**, **98** and **106**, of which the condensations of ortho-arylenediamine and dianhydride, anhydride, tetracarboxylicacid, dicarboxylicacid or 1,2-diketone usually performed in the heated organic solvents such as acetic acid, trifluoroacetic acid, polyphosphoric acid, ethanol, n-BuOH, imidazole, or HMPA.[129–133,168,169]

5. Relationship between the thin-film structure and the device performance

For OTFTs, the study on the relationship between the thin film structure and the device performance is very important and also quite challenging. Since this topic is beyond the scope of this review, we only choose to highlight some key points for the

relationship of the thin film structure and the device performance of n-type OSCs: (i) The molecular packing (the microstructure of thin film) and the thin film morphology play an important role in the air stability of n-channel OTFTs, and the dense molecular packing, good thin-film morphology with high crystallinity, large grain sizes, and low density of grain boundaries are positive kinetic factors for realizing ambient-stable n-channel OTFTs even the energetic factors of n-type are negative due to the high LUMO energies (> –4.0 eV).[29–33] (ii) There would be interplay between energetic and kinetic factors on the ambient stability of n-channel OTFTs, as revealed by Bao and coworkers for the active layer thickness-dependent device stability.[33] (iii) The combination of energetic factors (e.g. LUMO < –4.0 eV for n-type OSCs) and kinetic elements (e.g. dense molecular packing in solid state and good thin-film morphology) could realize long-term air stability for n-channel OTFTs.[36,125] (iv) The crystallinity and crystallite-growth direction of active thin film significantly affect the electron mobility and other device characteristics of n-channel OTFTs, the highly crystallized thin film with large domains, ordered grain orientation, and the dense molecular packing are highly desired for achieving high electron mobility.[22,37,38,102]

6. Conclusion and outlook

In the last decade, the development of n-type OSCs for OTFTs has witnessed great progress, hundreds of n-type small molecular and polymeric materials were designed and synthesized, some of which exhibited electron mobility comparable to or even higher than the mobility of amorphous silicon (0.5 ~ 1.0 $cm^2 V^{-1}s^{-1}$). Molecular design is the basic motive for developing n-type OSCs. We summarized more than

nine molecular design strategies and used the representative n-type OSCs to demonstrate each one. These molecular design strategies are generally effective for obtaining high-performance ambient-stable n-type OSCs for OTFTs, where the energetic and kinetic factors were considered for realizing the ambient-stable electron injection and transport. We envision that some new molecular design strategies would emerge in the future, but these strategies will continue to promote the development of n-type OSCs in the field of OTFTs

There are still some problems and challenges for the development of n-type OSCs for OTFTs, and special attention should be paid to these issues. (i) What govern the air/operating stability of n-channel OTFTs? The energetic/kinetic factors and their combination are still not enough to solve this problem. (ii) The pursuit of low-lying LUMO energy levels of n-type OSCs (such as < –4.0 eV) is not the only task for realizing ambient-stable n-channel OTFTs, since the HOMO energies should also be controlled (such as < –6.0 eV), otherwise the hole transport would appear, which goes against the pure n-channel charge transport. (iii) The device performance of current n-type OSCs is still lower than that of their p-type counterparts with unsatisfied device air/operating stability, especially for the pure electron-transport polymeric OSCs, where the performance was relied on the sandwiched TGBC device structure and/or the inert-atmosphere or vacuum testing conditions; the main indexes for next generation n-type OSCs for OTFTs would be $\mu_e \geq 5$ cm^2 V^{-1}s^{-1}, $I_{on/off} \geq 10^6$ and $|V_T| \leq 10$ V with easy processing property and excellent air/operating device stability. The following three points are important for both n-type OSCs and p-type ones: (iv) Most

solution-processed high-performance OTFTs depend on the utilization of chloro-carbon solvents such as chloroform, chlorobenzene and dichlorobenzene, while these chlorinated solvents are harmful to humans and the environment, the green non-chlorinated solvents are highly desirable for the real use of OSCs in printing electronics. (v) Solution-processable OSCs towards printing electronics do not always mean "the real low cost", the synthetic cost of the material itself should also be considered, facile and low-cost synthesis of OSCs with simple purification is also a significant topic in organic electronics. (vi) The integrated circuit technology using both n- and p-type OSCs is the most challenging topic, which is badly in need of the development of matching dielectric/electrode/substrate/interface-modification materials and techniques with current OSCs.

Acknowledgements

This work was financially supported by National Natural Science Foundation (20902105 and 51173200), MOST (2011CB932300), and the Chinese Academy of Sciences. We thank Simin Gao for helpful disscussions.

References

1 A. C. Arias, J. D. Mackenzie, I. McCulloch, J. Rivnay and A. Salleo, *Chem. Rev*., 2010, **110**, 3.

2 G. Gelinck, P. Heremans, K. Nomoto and T. Anthopoulos, *Adv. Mater*., 2010, **22**, 3778.

3 J. E. Anthony, A. Facchetti, M. Heeney, S. R. Marder and X. Zhan, *Adv. Mater*., 2010, **22**, 3876.

4 C. Wang, H. Dong, W. Hu, Y. Liu and D. Zhu, *Chem. Rev*., 2012, **112**, 2208.

5 H. Minemawari, T. Yamada, H. Matsui, J. Tsutsumi, S. Haas, R. Chiba, R. Kumai and T. Hasegawa, *Nature.*, **2011**, **475**, 364.

6 J. Li, Y. Zhao, H. Tan, Y. Guo, C. Di, G. Yu, Y. Liu, M. Lin, S. H. Lim, Y. Zhou, H. Su, B. S. Ong, *Sci. Rep.*, 2012, **2**, 754.

7 I. Kang, H.-J. Yun, D. S. Chung, S.-K. Kwon and Y.-H. Kim, *J. Am. Chem. Soc*., 2013, **135**, 14896.

8 J. Zaumseil and H. Sirringhaus, *Chem. Rev*., 2007, **107**, 1296.

9 L.-L. Chua, J. Zaumseil, J.-F. Chang, E. C.-W. Ou, P. K.-H. Ho, H. Sirringhaus and R. H. Friend, *Nature.*, 2005, **434**. 194.

10 J. Veres, S. Ogier, G. Lloyd and D. de Leeuw, *Chem. Mater*., 2004, **16**, 4543.

11 C. R. Newman, C. D. Frisbie, D. A. da Silva Filho, J.-L. Brédas, P. C. Ewbank and K. R. Mann, *Chem. Mater*., 2004, **16**, 4436.

12 C.-a. Di, Y. Liu, G. Yu and D. Zhu, *Acc. Chem. Res.*, 2009, **42**, 1573.

13 G. Guillaud, M. A. Sadoun and M. Maitrot, *Chem. Phys. Lett*., 1990, **167**, 503.

14 Y. Wen and Y. Liu, *Adv. Mater*., 2010, **22**, 1331.

15 B. J. Jung, N. J. Tremblay, M.-L. Yeh and H. E. Katz, *Chem. Mater*., 2011, **23**, 568.

16 X. Zhan, A. Facchetti, S. Barlow, T. J. Marks, M. A. Ratner, M. R. Wasielewshi and S. R. Marder, *Adv. Mater*., 2011, **23**, 268.

17 X. Zhang and X. Zhan, *Chem. Soc. Rev*., 2011, **40**, 3728.

18 Q. Meng and W. Hu, *Phys. Chem. Chem. Phys*., 2012, **14**, 14152.

19 S. Kola, J. Sinha and H. E. Katz, *J. Poly. Sci. Part B: Poly. Phys.*, 2012, **50**, 1090.

20 Y. Zhao, Y. Guo and Y. Liu, *Adv. Mater*., 2013, **25**, 5372.

21 D. M. de Leeuw, M. M. J. Simenon, A. R. Brown and R. E. F. Einerhand, *Syn. Met.*, 1997, **87**, 53.

22 D. Shukla, S .F. Nelson, D. C. Freeman, M. Rajeswaran, W. G. Ahearn, D. M. Meyer and J. T. Carey, *Chem. Mater*., 2008, **20**, 7486.

23 Z. Wang, C. Kim, A. Facchetti and T. J. Marks, *J. Am. Chem. Soc.*, 2007, **129**, 13362.

24 B. A. Jones, A. Facchetti, M. R. Wasielewski and T. J. Marks, *J. Am. Chem. Soc.*, 2007, **129**, 15259.

25 H. Usta, C. Risko, Z. Wang, H. Huang, M. K. Deliomeroglu, A. Zhukhovitskiy, A. Facchetti and T. J. Marks, *J. Am. Chem. Soc.*, 2009, **131**, 5586.

26 H. Usta, A. Facchetti and T. J. Marks, *Acc. Chem. Res.*, 2011, **44**, 501.

27 T. D. Anthopoulos, F. B. Kooistra, H. J. Wondergem, D. Kronholm, J. C. Hummelen and D. M. de Leeuw, *Adv. Mater*., 2006, **18**, 1679.

28 Z. Bao, A. J. Lovinger and J. Brown, *J. Am. Chem. Soc.*, 1998, **120**, 207.

29 H. E. Katz, A. J. Lovinger, J. Johnson, C. Kloc, T. Siegrist, W. Li, Y.-Y. Lin and A. Dodabalapur, *Nature.*, 2000, **404**, 478.

30 H. E. Katz, J. Johnson, A. J. Lovinger and W. Li, *J. Am. Chem. Soc.*, 2000, **122**, 7787.

31 M.-M. Ling, P. Erk, M. Gomez, M. Koenemann, J. Locklin and Z. N. Bao, *Adv. Mater.*, 2007, **19**, 1123.

32 R. T. Weitz, K. Amsharov, U. Zschieschang, M. Burghard, M. Jansen, M. Kelsch,

B. Rhamati, P. A. Van Aken, K. Kern and H. Klauk, *Chem. Mater*., 2009, **21**, 4949.

33 J. H. Oh, Y.-S. Sun, R. Schmidt, M. F. Toney, D. Nordlund, M. Könemann, F. Würthner and Z. Bao, *Chem. Mater*., 2009, **21**, 5508.

34 A. Facchetti, Y. Deng, A. Wang, Y. Koide, H. Sirringhaus, T. J. Marks and R. H. Friend, *Angew. Chem. Int. Ed*., 2000, **39**, 4547.

35 Y. Sakamoto, T. Suzuki, M. Kobayashi, Y. Gao, Y. Fukai, Y. Inoue, F. Sato and S. Tokito, *J. Am. Chem. Soc.*, 2004, **126**, 8138.

36 B. A. Jones, M. J. Ahrens, M.-H. Yoon, A. Facchetti, T. J. Marks and M. R. Wasielewski, *Angew. Chem. Int. Ed*., 2004, **43**, 6363.

37 C. Piliego, D. Jarzab, G. Gigli, Z. Chen, A. Facchetti and M. A. Loi, *Adv. Mater.*, 2009, **21**, 1573.

38 J. Soeda, T. Uemura, Y. Mizuno, A. Nakao, Y. Nakazawa, A. Facchetti and J. Takeya, *Adv. Mater.*, 2011, **23**, 3681.

39 A. S. Molinari, H. Alves, Z. Chen, A. Facchetti and A. F. Morpurgo, *J. Am. Chem. Soc.*, 2009, **131**, 2462.

40 N. A. Minder, S. Ono, Z. Chen, A. Facchetti and A. F. Morpurgo, *Adv. Mater.*, 2012, **24**, 503.

41 R. T. Weitz, K. Amsharov, U. Zschieschang, E. B. Villas, D. K. Goswami, M. Burghard, H. Dosch, M. Jansen, K. Kern and H. Klauk, *J. Am. Chem. Soc.*, 2008, **130**, 4637.

42 S. V. Bhosale, C. H. Jani and S. J. Langford, *Chem. Soc. Rev*., 2008, **37**, 331.

43 Z. Zhao, F. Zhang, X. Zhang, X. Yang, H. Li, X. Gao, C.-a. Di and D. Zhu, *Macromolecules*., 2013, **46**, 7705.

44 B. J. Jung, K. Lee, J. Sun, A. G. Andreou and H. E. Katz, *Adv. Funct. Mater.*, 2010, **20**, 2930.

45 K. C. See, C. Landis, A. Sarjeant and H. E. Katz, *Chem. Mater.*, 2008, **20**, 3609.

46 B. J. Jung, J. Sun, T. Lee, A. Sarjeant and H. E. Katz, *Chem. Mater.*, 2009, **21**, 94.

47 Y. Jung, K. J. Baeg, D. Y. Kim, T. Someya and S. Y. Park, *Syn. Met.*, 2009, **159**, 2117.

48 H. Chen, M. Ling, X. Mo, M. Shi, M. Wang and Z. Bao, *Chem. Mater.*, 2007, **19**, 816.

49 R. Schmidt, J. H. Oh, Y. S. Sun, M. Deppisch, A. M. Krause, K. Radacki, H. Braunschweig, M. Konemann, P. Erk, Z. A. Bao and F. Würthner, *J. Am. Chem. Soc*., 2009, **131**, 6215.

50 Q. Zheng, J. Huang, A. Sarjeant and H. E. Katz, *J. Am. Chem. Soc.*, 2008, **130**, 14410.

51 S Chen, Q. Zhang, Q. Zheng, C. Tang and C. Lu, *Chem. Commun.*, 2012, **48**, 1254.

52 S.-C. Chen, D. Ganeshan, D. Cai, Q. Zheng, Z. Yin and F. Wang, *Org. Electron.*, 2013, **14**, 2859.

53 M. Chikamatsu, A. Itakura, Y. Yoshida, R. Azumi and K. Yase, *Chem. Mater.*, 2008, **20**, 7365.

54 Y. Ie, M. Ueta, M. Nitani, N. Tohnai, M. Miyata, H. Tada and Y. Aso, *Chem.*

Mater., 2012, **24**, 3285.

55 Y. I. Park, J. S. Lee, B. J. Kim, B. Kim, J. Lee, D. H. Kim, S. Y. Oh, J. H. Cho and J. W. Park, *Chem. Mater.*, 2011, **23**, 4038.

56 C. Di, J. Li, G. Yu, Y. Xiao, Y. Guo, Y. Liu, X. Qian and D. Zhu, *Org. Lett.*, 2008, **10**, 3025.

57 B. A. Jones, A. Facchetti, T. J. Marks and M. R. Wasielewski, *Chem. Mater.*, 2007, **19**, 2703.

58 B. Yoo, B. A. Jones, D. Basu, D. Fine, T. Jung, S. Mohapatra, A. Facchetti, K. Dimmler, M. R. Wasielewski, T. J. Marks and A. Dodabalapur, *Adv. Mater.*, 2007, **19**, 4028.

59 H. Yan, Y. Zheng, R. Blache, C. Newman, S. F. Lu, J. Woerle and A. Facchetti, *Adv. Mater.*, 2008, **20**, 3393.

60 J. Chang, H. Qu, Z.-E. Ooi, J. Zhang, Z. Chen, J. Wu and C. Chi, *J. Mater. Chem. C.*, 2013, **1**, 456.

61 J. Li, J.-J. Chang, H. S. Tan, H. Jiang, X. Chen, Z. Chen, J. Zhang and J. Wu, *Chem. Sci.*, 2012, **3**, 846.

62 W. Hong, C. Guo, B. Sun, Z. Yan, C. Huang, Y. Hu, Y. Zheng, A. Facchetti and Y. Li, *J. Mater. Chem. C.*, 2013, **1**, 5624.

63 M. Gsänger, J. H. Oh, M. Konemann, H. W. Hoffken, A. M. Krause, Z. N. Bao and F. Würthner, *Angew. Chem. Int. Ed.*, 2010, **49**, 740.

64 Y. Li, L. Tan, Z. H. Wang, H. L. Qian, Y. B. Shi and W. P. Hu, *Org. Lett.*, 2008, **10**, 529.

65 Y. Takeda, T. L. Andrew, J. M. Lobez, A. J. Mork and T. M. Swager, *Angew. Chem.*

Int. Ed., 2012, **51**, 9042.

66 M. Mamada, D. Kumaki, J. Nishida, S. Tokito and Y. Yamashita, *Acs. Appl. Mater. Inter.*, 2010, **2**, 1303.

67 S. Chen, Y. Zhao, A. Bolag, J. Nishida, Y. Liu and Y. Yamashita, *Acs. Appl. Mater. Inter.*, 2012, **4**, 3994.

68 H. Usta, C. Kim, Z. M. Wang, S. F. Lu, H. Huang, A. Facchetti and T. J. Marks, *J. Mater. Chem.*, 2012, **22**, 4459.

69 R. Schmidt, M. M. Ling, J. H. Oh, M. Winkler, M. Konemann, Z. N. Bao and F. Würthner, *Adv. Mater.*, 2007, **19**, 3692.

70 M. L. Tang, J. H. Oh, A. D. Reichardt and Z. N. Bao, *J. Am. Chem. Soc.*, 2009, **131**, 3733.

71 J. H. Oh, S. L. Suraru, W. Y. Lee, M. Konemann, H. W. Hoffken, C. Roger, R. Schmidt, Y. Chung, W. C. Chen, F. Würthner and Z. N. Bao, *Adv. Funct. Mater.*, 2010, **20**, 2148.

72 M. Stolte, M. Gsanger, R. Hofmockel, S. L. Suraru and F. Würthner, *Phys. Chem. Chem. Phys.*, 2012, **14**, 14181.

73 T. He, M. Stolte and F. Würthner, *Adv. Mater.*, 2013, DOI:10.1002/adma. 201303392.

74 A. Facchetti, *Chem. Mater.*, 2011, **23**, 733.

75 X. Zhan, Z. Tan, B. Domercq, Z. An, X. Zhang, S. Barlow, Y. Li, D. Zhu, B. Kippelen and S. R. Marder, *J. Am. Chem. Soc.*, 2007, **129**, 7246.

76 X. Zhao, L. Ma, L. Zhang, Y. Wen, J. Chen, Z. Shuai, Y. Liu and X. Zhan,

Macromolecules., 2013, **46**, 2152.

77 X. Zhao, Y. Wen, L. Ren, L. Ma, Y. Liu and X. Zhan, *J. Polym. Sci. Pol. Chem.*, 2012, **50**, 4266.

78 S. G. Hahm, Y. Rho, J. Jung, S. H. Kim, T. Sajoto, F. S. Kim, S. Barlow, C. E. Park, S. A. Jenekhe, S. R. Marder and M. Ree, *Adv. Funct. Mater.*, 2013, **23**, 2060.

79 Z. Chen, Y. Zheng, H. Yan and A. Facchetti, *J. Am. Chem. Soc*., 2009, **131**, 8.

80 H. Yan, Z. Chen, Y. Zheng, C. Newman, J. R. Quinn, F. Dotz, M. Kastler and A. Facchetti, *Nature.*, 2009, **457**, 679.

81 H. Huang, Z. Chen, R. P. Ortiz, C. Newman, H. Usta, S. Lou, J. Youn, Y. Y. Noh, K. J. Baeg, L. Chen, A. Facchetti and T. J. Marks, *J. Am. Chem. Soc.*, 2012, **134**, 10966.

82 M. M. Durban, P. D. Kazarinoff and K. Luscombe, *Macromolecules*., 2010, **43**, 6348.

83 M. Yuan, M. M. Durban, P. D. Kazarinoff, D. F. Zeigler, A. H. Rice, Y. Segawa and C. K. Luscombe, *J. Polym. Sci. Pol. Chem.*, 2013, **51**, 4061.

84 X. Guo, F. S. Kim, M. J. Seger, S. A. Jenekhe and M. D. Watson, *Chem. Mater.*, 2012, **24**, 1434.

85 Y. Kim, J. Hong, J. H. Oh and C. Yang, *Chem. Mater.*, 2013, **25**, 3251.

86 H. Chen, Y. Long, Z. Mao, G. Yu, J. Huang, Y. Zhao and Y. Liu, *Chem. Mater.*, 2013, **25**, 3589.

87 R. Kim, P. S. K. Amegadze, I. Kang, H.-J. Yun, Y.-Y. Noh, S.-K. Kwon and Y.-H. Kim, *Adv. Funct. Mater.*, 2013, DOI: 10.1002/adfm.201301197.

88 Y.-J. Hwang, G. Ren, N. M. Murari and S. A. Jenekhe, *Macromolecules*., 2012, **45**, 9056.

89 Y.-J. Hwang, N. M. Murari and S. A. Jenekhe, *Polym. Chem.-Uk.*, 2013, **4**, 3187.

90 H. Li, F. S. Kim, G. Ren and S. A. Jenekhe, *J. Am. Chem. Soc*., 2013, **135**, 14920.

91 C. Kanimozhi, N. Yaacobi-Gross, K. W. Chou, A. Amassian, T. D. Anthopoulos and S. Patil, *J. Am. Chem. Soc*., 2012, **134**, 16532.

92 J. H. Park, E. H. Jung, J. W. Jung and W. H. Jo, *Adv. Mater.*, 2013, **25**, 2583.

93 L. Tan, Y. Guo, G. Zhang, Y. Yang, D. Zhang, G. Yu, W. Xu and Y. Liu, *J. Mater. Chem.*, 2011, **21**, 18042.

94 Y. Fukutomi, M. Nakano, J. Y. Hu, I. Osaka and K. Takimiya, *J. Am. Chem. Soc*., 2013, **135**, 11445.

95 L. E. Polander, S. P. Tiwari, L. Pandey, B. M. Seifried, Q. Zhang, S. Barlow, C. Risko, J. L. Bredas, B. Kippelen and S. R. Marder, *Chem. Mater.*, 2011, **23**, 3408.

96 D. K. Hwang, R. R. Dasari, M. Fenoll, V. Alain-Rizzo, A. Dindar, J. W. Shim, N. Deb, C. Fuentes-Hernandez, S. Barlow, D. G. Bucknall, P. Audebert, S. R. Marder and B. Kippelen, *Adv. Mater.*, 2012, **24**, 4445.

97 X. Gao, C. Di, Y. Hu, X. Yang, H. Fan, F. Zhang, Y. Liu, H. Li and D. Zhu, *J. Am. Chem. Soc*., 2010, **132**, 3697.

98 Y. Hu, X. Gao, C. Di, X. Yang, F. Zhang, Y. Liu, H. Li and D. Zhu, *Chem. Mater*., 2011, **23**, 1204.

99 Y. Hu, Y. Qin, X. Gao, F. Zhang, C. Di, Z. Zhao, H. Li and D. Zhu, *Org. Lett*., 2012, **14**, 292.

100 Y. Hu, Z. Wang, X. Zhang, X. Yang, H. Li and X. Gao, *Chin. J. Chem*., 2013, **31**, 1428.

101 Y. Zhao, C. Di, X. Gao, Y. Hu, Y. Guo, L. Zhang, Y. Liu, J. Wang, W. Hu and D. Zhu, *Adv. Mater*., 2011, **23**, 2448.

102 F. Zhang, Y. Hu, T. Schuettfort, C. Di, X. Gao, C. R. McNeill, L. Thomsen, S. C. B. Mannsfeld, W. Yuan, H. Sirringhaus and D. Zhu, *J. Am. Chem. Soc*., 2013, **135**, 2338.

103 F. Zhang, C. Di, N. Berdunov, Y. Hu, Y. Hu, X. Gao, Q. Meng, H. Sirringhaus and D. Zhu, *Adv. Mater*., 2013, **25**, 1401.

104 X. Gao, J. Dou, D. Li, F. Dong and D. Wang, *J. Chem. Crystallogr.,* 2005, **35**, 107.

105 X. Gao, J. Dou, D. Li, F. Dong and D. Wang, *J. Incl. Phen. Macro. Chem*., 2005, **53**, 111.

106 X. Gao, W. Qiu, X. Yang, Y. Liu, Y. Wang, H. Zhang, T. Qi, Y. Liu, K. Lu, C. Du, Z. Shuai, G. Yu and D. Zhu, *Org. Lett.*, 2007, **9**, 3917.

107 Y. Yamashita, T. Suzuki, G. Saito and T. Mukai, *J. Chem. Soc., Chem. Commun.*, 1986, 1489.

108 T. Lei, J.-H. Dou and J. Pei, *Adv. Mater*., 2012, **24**, 6457.

109 Z. Qi, X. Liao, J. Zheng, C. Di, X. Gao and J. Wang, *Appl. Phys. Lett*., 2013, **103**, 0553301.

110 X. Chen, Y. Guo, L. Tan, G. Yang, Y. Li, G. Zhang, Z. Liu, W. Xu and D. Zhang, *J. Mater. Chem. C.*, 2013, **1**, 1087.

111 H. Luo, Z. Cai, L. Tan, Y. Guo, G. Yang, Z. Liu, G. Zhang, D. Zhang, W. Xu and Y. Liu, *J. Mater. Chem. C.*, 2013, **1**, 2688.

112 X. Chen, J. Wang, G. Zhang, Z. Liu, W. Xu and D. Zhang, *New. J. Chem.*, 2013, **37**, 1720.

113 A. R. Brown, D. M. de Leeuw, E. J. lous and E. E. Havinga, *Synth. Met*., 1994, **66**, 257.

114 M. Yamagishi, Y. Tominari, T. Uemura and J. Takeya, *Appl. Phys. Lett.*, 2009, **94**, 053305.

115 T. M. Pappenfus, R. J. Chesterfield, C. D. Frisbie, K. R. Mann, J. Casado, J. D. Raff and L. L. Miller, *J. Am. Chem. Soc.*, 2002, **124**, 4184.

116 R. J. Chesterfield, C. R. Newman, T. M. Pappenfus, P. C. Ewbank, M. H. Haukaas, K. R. Mann, L. L. Miller and C. D. Frisbie, *Adv. Mater.*, 2003, **15**, 1278.

117 S. Handa, E. Miyazaki, K. Takimiya and Y. Kunugi, *J. Am. Chem. Soc*., 2007, **129**, 11684.

118 Y. Suzuki, E. Miyazaki and K. Takimiya, *J. Am. Chem. Soc*., 2010, **132**, 10453.

119 Y. Suzuki, M. Shimawaki, E. Miyazaki, I. Osaka and K. Takimiya, *Chem. Mater.*, 2011, **23**, 795.

120 Q. Wu, R. Li, W. Hong, H. Li, X. Gao and D. Zhu, *Chem. Mater.*, 2011, **23**, 3138.

121 Q. Wu, S. Ren, M. Wang, X. Qiao, H Li, X. Gao, X. Yang and D. Zhu, *Adv. Funct. Mater.*, 2013, **23**, 2277.

122 Y. Qiao, Y. Guo, C. Yu, F. Zhang, W. Xu, Y. Liu and D. Zhu, *J. Am. Chem. Soc.*,

2012, **134**, 4084.

123 H. Zhong, J. Smith, S. Rossbauer, A. J. P. White, T. D. Anthopoulos and M. Heeney, *Adv. Mater.*, 2012, **24**, 3205.

124 A. Babel and S. A. Jenekhe, *J. Am. Chem. Soc*., 2003, **125**, 13656.

125 A. L. Briseno, F. S. Kim, A. Babel, Y. Xia and S. A. Jenekhe, *J. Mater. Chem*., 2011, **21**, 16461.

126 M. M. Durban, P. D. Kazarinoff, Y. Segawa and C. K. Luscombe, *Macromolecules*., 2011, **44**, 4721.

127 C. W. Tang, *Appl. Phys. Lett.*, 1986, **48**, 183.

128 P. Dhagat, H. M. Haverinen, R. J. Kline, Y. Jung, D. A. Fischer, D. M. DeLongchamp and G. E. Jabbour, *Adv. Funct. Mater*., 2009, **19**, 2365.

129 R. P. Ortiz, H. Herrera, R. Blanco, H. Huang, A. Facchetti, T. J. Marks, Y. Zheng and J. L. Segura, *J. Am. Chem. Soc*., 2010, **132**, 8440.

130 P. Deng, Y. Yan, S.-D. Wang, Q. Zhang, *Chem. Commun*., 2012, **48**, 2591.

131 J. Chang, J. Shao, J. Zhang, J. Wu and C. Chi, *RSC. Adv*., 2013, **3**, 6775.

132 M. Zhu, J. Zhang, G. Yu, H. Chen, J. Huang and Y. Liu, *Chem. Asian. J.*, 2012, **7**, 2208.

133 H. Li, F. S. Kim, G. Ren, E. C. Hollenbeck, S. Subramaniyan and S. A. Jenekhe, *Angew. Chem. Int. Ed*., 2013, **52**, 5513.

134 L. E. Polander, A. S. Romanov, S. Barlow, D. K. Hwang, B. Kippelen, T. V. Timofeeva and S. R. Marder, *Org. Lett*., 2012, **14**, 918.

135 J. A. Letizia, M. R. Salata, C. M. Tribout, A. Facchetti, M. A. Ratner and T.

Marks, *J. Am. Chem. Soc*., 2008, **130**, 9679.

136 X. Guo, R. P. Ortiz, Y. Zheng, Y. Hu, Y.-Y. Noh, K.-J. Baeg, A. Facchetti and T. Marks, *J. Am. Chem. Soc*., 2011, **133**, 1405.

137 T. Lei, J.-H. Dou, X.-Y. Cao, J.-Y. Wang and J. Pei, *J. Am. Chem. Soc*., 2013, **135**, 12168.

138 S. Kola, J. H. Kim, R. Ireland, M.-L. Yeh, K. Smith, W. Guo and H. E. Katz, *ACS. Macro. Lett*., 2013, **2**, 664.

139 S. K. Park, J. H. Kim, S.-J. Yong, O. K. Kwon, B.-K. An and S. Y. Park, *Chem. Mater*., 2012, **24**, 3263.

140 A. Lv, S. R. Puniredd, J. Zhang, Z. Li, H. Zhu, W. Jiang, H. Dong, Y. He, L. Jiang, Y. Li, W. Pisula, Q. Meng, W. Hu and Z. Wang, *Adv. Mater*., 2011, **24**, 2626.

141 J. Zhang, L. Tan, W. Jiang, W. Hu and Z. Wang, *J. Mater. Chem. C*., 2013, **1**, 3200.

142 W. Yue, A. Lv, J. Gao, W. Jiang, L. Hao, C. Li, Y. Li, L. E. Polander, S. Barlow, W. Hu, S. D. Motta, F. Negri, S. R. Marder and Z. Wang, *J. Am. Chem. Soc*., 2012, **134**, 5770.

143 X. Li, C. Xiao, W. Jiang and Z. Wang, *J. Mater. Chem. C*., 2013, **1**, 7513.

144 D. Song, H. Wang, F. Zhu, J. Yang, H. Tian, Y. Geng and D. Yan, *Adv. Mater*., 2008, **20**, 2142.

145 D. Song, F. Zhu, B. Yu, L. Huang, Y. Geng and D. Yan, *Appl. Phys. Lett*., 2009, **92**, 143303.

146 C. Pearson. J. E. Gibson. A. J. Moore, R. M. Bryce and M. C. Petty, *Electron. Lett.*, 1993, **29**, 1377.

147 H. Wada, T. Taguchi, B. Noda, T. Kambayashi, T. Mori, K. Ishikawa and H. Takezoe, *Org. Electron*., 2007, **8**, 759.

148 L. Qu, Y. Guo, H. Luo, C. Zhong, G. Yu, Y. Liu and J. Qin, *Chem. Commun*., 2012, **48**, 9965.

149 J.-Y. Cho, B. Domercq, S. C. Jones, J. Yu, X. Zhang, Z. An, M. Bishop, S. Barlow, S. R. Marder and B. Kippelen, *J. Mater. Chem*., 2007, **17**, 2642.

150 T. Inabe and H. Tajima, *Chem. Rev*., 2004, **104**, 5503.

151 A. Kobayashi, E. Fujiwara and H. Kobayashi, *Chem. Rev*., 2004, **104**, 5243.

152 R. Kato, *Chem. Rev*., 2004, **104**, 5319.

153 Z. Liang, Q. Tang, J. Liu, J. Li, F. Yan and Q. Miao, *Chem. Mater.,* 2010, **22**, 6438.

154 Z. Liang, Q. Tang, J. Xu and Q. Miao, *Adv. Mater.*, 2011, **23**, 1535.

155 D. Liu, X. Xu, Y. Su, Z. He, J. Xu and Q. Miao, *Angew. Chem. Int. Ed.*, 2013, **52**, 6222.

156 M. M. Islam, S. Pola and Y.-T. Tao, *Chem. Commun*., 2011, **47**, 6356.

157 S. M. Lindner and M. Thelakkat, *Macromolecules*., 2004, **37**, 8832.

158 S. Hüttner, M. Sommer and M. Thelakkat, *Appl. Phys. Lett.,* 2008, **92**, 093302.

159 C. Huang, W. J. P. Jr, S. P. Tiwari, S. Sutcu, S. Barlow, B. Kippelen and S. R. Marder, *Polym. Chem*., 2012, **3**, 2996.

160 A. Pron, P. Gawrys, M. Zagorska, D. Djurado and R. Demadrille, *Chem. Soc.*

Rev., 2010, **39**, 2577.

161 M. J. Ahrens, M. J. Fuller and M. R. Wasielewski, *Chem. Mater*., 2003, **15**, 2684.

162 B. Carsten, F. He, H. J. Son, T. Xu and L. Yu, *Chem. Rev*., 2011, **111**, 1493.

163 Y. Hu, Z. Wang, X. Yang, Z. Zhao, W. Han, W. Yuan, H. Li, X. Gao and D. Zhu, *Tetrahedron. Lett*., 2013, **54**, 2271.

164 W. Yue, J. Gao, Y. Li, W. Jiang, S. D. Motta, F. Negri and Z. Wang, *J. Am. Chem. Soc*., 2011, **133**, 18054.

165 Q. Ye, J. Chang, K.-W. Huang and C. Chi, *Org. Lett*., 2011, **13**, 5960.

166 L. Tan, Y. Guo, Y. Yang, G. Zhang, D. Zhang, G. Yu, W. Xu and Y. Liu, *Chem. Sci*., 2012, **3**, 2530.

167 K. Cai, Q. Yan and D. Zhao, *Chem. Sci*., 2012, **3**, 3175.

168 F. E. Arnold and R. L. Van Deusen, *Macromolecules*., 1969, **2**, 497.

169 J. K. Stille and E. L. Mainen, *Macromolecules*., 1968, **1**, 36.

TOC

More than nine molecular design strategies with > 120 representative n-type organic semiconductors were summarized and analyzed.